A Differentiation Therapy for the N2a Neuroblastoma

through the Cholesterol Synthesis Pathway

by

Paul R. Hollis

A Thesis Submitted in Partial Fulfillment
of the Requirements for the Degree for the
Master of Science in Biology

Middle Tennessee State University

August 2013

Thesis Committee:

William C. Stewart

Anthony Farone

Matthew Elrod-Erickson

ABSTRACT

Neuroblastomas are the second most common childhood cancer, claiming 15% of all childhood cancer deaths. To discover a differentiation therapy to treat the cancerous neuroblastoma cell, the elevated activity of the cholesterol synthesis pathway has been investigated. Statin drugs are aggressive inhibitors of the rate limiting enzyme, HMG-CoA reductase, of the cholesterol synthesis pathway. Inhibition of this enzyme eliminates the production of downstream intermediates, along with their entire non-sterol and sterol end products. Add-back experiments exposed that mevinolin co-treatment with cholesterol intermediates mevalonate, farnesyl pyrophosphate, and geranylgeranyl pyrophosphate, blocked neurite outgrowths and cells appear unable to differentiate, exhibiting the typical morphology of neuroblastoma cells. However, the add-back of cholesterol (dissolved in 95% ethanol) triggered differentiation of the N2a neuroblastoma cell. This study demonstrates that the N2a neuroblastoma cell differentiates after add-back of cholesterol, implying that the agent(s) of differentiation lies above the production of cholesterol.

TABLE OF CONTENTS

Page

LIST OF FIGURES

LIST OF TABLES

INTRODUCTION

Neuroblasts are nascent nerve cells, derived from the neural crest, that receive signals to migrate, leading to the development of a sympathetic, post-synaptic neuron of the autonomic nervous system. When molecular defects occur causing malignant mutations, the neuroblasts lose control of cellular growth, outgrowing tissue restraints and fail to produce mature nerve cells or adrenal medullary cells. The continuous division and rapid overgrowth of cells will then produce a tumor that contains undifferentiated neuroectodermal cells (Brodeur 2003). The tumors are termed neuroblastomas and can spread to all areas in the body where the sympathetic chain resides. The enigmatic neuroblastoma maintains the position as the second most common childhood cancer (Evangelopoulous 2009), credited to 7-10% of all pediatric cancers (Brodeur 2003), and the extracranial tumor comprises 15% of infantile deaths (Riley 2004). Alluding to their enigmatic nature, neuroblastoma cells can undergo unexpected behaviors of excessive metastatic growth, or even exhibit spontaneous regression by way of differentiation or apoptosis (Riley 2004). Common symptoms of neuroblastomas are an unusually large mass or nodule. These masses can reach a size that can occlude brain, neck, adrenal gland, and internal organ functions, causing excessive swelling or can be found in the skin, indicated by blue or purple bruising (Simpson 1998).

The unexpected malignant mutation provoked by molecular defects is thought to disrupt signaling pathways, hindering the advancement of these immature nerve cells into sympathetic neurons (Evangelopoulos 2009). A common attribute that is found in cancer

cells, due to the malignant mutation, is the elevated activity of the cholesterol synthesis pathway. The appearance of increased levels of HMG-CoA reductase results in the unregulated activity of the cholesterol synthesis pathway has been reported in neuroblastoma cells (Maltese 1985) as well as multiple types of malignant cells such as lymphoma, leukemia, hepatocellular carcinoma, and colorectal adenocarcinoma (Wong 2002). Due to the irregular activity of the HMG-CoA reductase, questions loomed whether the elevated activity of the cholesterol synthesis pathway was responsible for the formation of the neuroblastoma cell.

The cholesterol synthesis pathway is a vital pathway that is instrumental to maintaining cellular integrity, supplying cells with important bioactive molecules that regulate multiple cellular procedures (Buhaescu 2007). In normal cells, for the pathway to operate effectively, protective feedback loops are integrated to regulate and maintain appropriate levels of sterol and non-sterol products, establishing the pathway as a "multivalent" system (Cohen 1982). Regulation of the pathway is maintained by negative feedback loops from both the sterol and non-sterol isoprenoid intermediates (Nakanishi 1988). The HMG-CoA reductase, as well as the LDL receptor, gene transcription is regulated by the feedback loop of sterols, whereas translation of HMG-CoA reductase mRNA is regulated by non-sterol isoprenoid intermediates (Dawson 1991). The regulatory feedback control of HMG-CoA reductase is an effective means to govern the rate of mevalonate production, preventing continuous activation and accumulation of end products in the cholesterol synthesis pathway. Procession downstream, the cholesterol synthesis pathway produces several, biologically active

intermediates. Each intermediate leads to the production of subsequent intermediates, which produce sterol and non-sterol end products, as shown in Fig. 1. Farnesyl pyrophosphate (FPP) can be modified to produce dolichol, a carrier molecule essential for protein glycosylation forming glycoproteins (Chan 2003). Further FPP modification leads to ubiquinone, which participates in electron transport chain (Wong 2002), and heme A, which functions in cell respiration. (van de Donk 2002). FPP modification also produces geranygeranyl pyrophosphate (DeBose-Boyd 2008). Prenylation by farnesyl and geranylgeranyl groups facilitates post translational modification of G-proteins to cell membranes by enabling attachment, anchoring, and membrane localization of protein-lipid and protein-protein interactions (Cordle 2005, Vamvakopoulos 2005). The prenylation of proteins is crucial to the function of the G-proteins i.e. Rho, Ras, Rab, Rac, and Rap (Chan 2003, Dimiere 2005, Kuipers 2007). Ultimately, farnesyl pyrophosphate is converted to cholesterol, the sterol isoprenoid. Cholesterol is a crucial molecule that sustains membrane structural integrity, and can be converted to vitamin D, bile acid, and steroid hormone production (Li 2003, Vamvakopoulos 2005). Prenylated proteins, as well as cholesterol, control cell proliferation, signal transduction, cytoskeletal reorganization, cell-to-cell communication, endocytosis and exocytosis (Chan 2003, Buhaescu 2007). Due to the malignant mutations in cancer cells, the regulatory mechanisms are lost that control the cholesterol synthesis pathway in cancer cells (Siperstein 1984, Buchwald 1992). Continuous activation, with large amounts of downstream end products supporting the cellular membranes' excessive growth and

expansion that is required characteristic of cancer cells (Buchwald 1992, Fernandez 2004).

Statin drugs are aggressive inhibitors of the cholesterol synthesis pathway. They competitively bind to the rate limiting enzyme, HMG-CoA reductase, preventing production of the cholesterol synthesis pathway (Demierre 2005, Pooler 2006, Evangelopoulos 2009, Martini 2009). Clinically, statins are a widely prescribed family of drugs generally used to treat hypercholesterolemia, effectively decreasing cholesterol levels and preventing cardiovascular disease (Chan 2003, Kuipers 2007). Interestingly, patients taking statins show a reduced risk of developing cancer (Chan 2003). Statin treatment appears to inhibit cell growth (Sanchez-Martin 2007). The most effectual statin chemical structure contains an open ring that permits binding to the active site of the HMG-CoA reductase enzyme, blocking the attachment HMG-CoA and activation of the first committed step of the pathway, mevalonate (Schachter 2004), exhibiting an increased binding affinity for HMG-CoA reductase than HMG-CoA (Vamvakopoulos 2005). Statins have been linked to cell cycle arrest, specifically in the G_1 phase, which is indicative of a mitotically inactive, growth suppressed cell and is required before differentiation can proceed (Jakobisiak 1991, Keyomarsi 1991, van de Donk 2002, Fernandez 2004, Vamvakopoulos 2005).

Present cancer treatments are a non-tumor specific, toxic therapy that treats cancer cells by triggering DNA damage. These treatments do not take into account whether the

cell death is from healthy, growing cells or cancerous tissue. The most common non-specific therapies are chemotherapy and radiation therapy (Leszcyniecka 2001). Neither treatment with chemotherapy, which uses the application of drugs to remove rapidly dividing cells, nor radiation therapy, which uses radiation to kill cancer cells, uses a specific approach to only kill cancer cells or the tumor. Chemotherapy is commonly correlated with drug resistance of cancer cells due to the combination of drugs given during treatment (Leszcyniecka 2001). These non-specific treatments induce detrimental side effects to the body including skin changes, fatigue, loss of appetite, hair loss, and nausea.

Differentiation therapy is a new, alternative approach that proposes a tumor specific therapy that is less harmful to surrounding, fast-dividing cells. This new therapy would eliminate the side effects and drug resistance that is commonly associated with chemotherapy and radiation therapy. By taking this specific approach, many cancer cell types experiencing defects in differentiation can be reversed, with cells undergoing tumor reprogramming to stimulate terminal differentiation. This study concentrated on the up-regulated activity of the cholesterol synthesis pathway, searching for the agent of differentiation. The hypothesis of this thesis is that the inhibition of the cholesterol synthesis pathway will induce differentiation due to the absence of cholesterol and/or cholesterol intermediates. Treatment of the pathway with intermediate substitution will assist in determining the agent of differentiation, delivering a potential differentiation therapy.

METHODS AND MATERIALS

Materials

The murine neuroblastoma (N2a) cells were purchased from the ATCC. Tissue culture treated flasks (25cm² and 75cm²), DMEM/Ham's F-12, 50/50 Mix with L-glutamine, MEM vitamins 100X solution, 10,000 IU penicillin, 10,000ug/mL streptomycin, 0.25% Trypsin+0.1% EDTA were purchased from Fisher. Fetal Bovine Serum (FBS) was purchased from Atlanta Biologicals. Phosphate Buffered Saline was purchased from Mediatech-Cellgro. Reagents mevinolin, mevalonolactone, 2-Hydroxypropyl-β-cyclodextrin, cholesterol, farnesyl pyrophosphate ammonium salt, and geranylgeranyl pyrophosphate ammonium salt were all purchased from Sigma Aldrich. The polyclonal AChE (82kDa) antibody was purchased from Santa Cruz Biotechnology. p38 MAPK (42/44 kDa) antibody was purchased from Cell Signalling Technology. Anti-NeuN (62, 46/48 kDa) monoclonal antibody was purchased from Millipore. Secondary antibodies were conjugated with horseradish peroxidase were purchased from Jackson Immunoresearch Laboratories.

Cell Culture

The murine neuroblastoma (N2a) cell line was used as the experimental model. N2a cells were grown in 25cm² cell culture flasks in culture medium mixture of Dulbecco's Modified Eagle's Medium and Ham's F-12 (DMEM/F-12 50/50). Media was supplemented with 10% heat inactivated fetal bovine serum (FBS), 1% Eagles vitamins, 100 IU/ml penicillin, and 100μg/ml of streptomycin. Grown in a monolayer, the cells

were placed in an incubator at 37˚C in a 5% CO_2 atmosphere. For sub-culturing, the monolayer of cells were exposed to 0.25% trypsin + 0.1% EDTA when cells had reached 90% confluence. Deactivation of trypsin was performed by suspending the cells in culture medium. Every third sub-culturing, cells were seeded in a new 25cm² flask. Number of cells to plate for 35mm and 100mm dishes was determined by using a Bright-Line hemacytometer. Passage number of cells for experiments were retained to <40.

Preparation of Reagents and Experimental Procedures

Mevinolin was solubilized in DMSO to 24.7mM and diluted in culture medium (0% FBS) to 2.47mM. Mevalonolactone (0.726M) was diluted in culture medium (0% FBS) to 29.04mM. Stock solutions and treatment solutions were stored at 4ºC. Farnesyl pyrophosphate (FPP) and geranylgeranyl pyrophosphate (GGPP) were purchased and delivered in liquid form in methanol:ammonia stock solution and stored at -20ºC. Stock solution of cholesterol was prepared by being solubilized in 95% ethanol to 20mM and diluted in culture medium (10% FBS) with a treatment concentration of 0.143mM. 10mM 2-hydroxypropyl-β-cyclodextrin (CD) stock solution was prepared by solubilizing in culture medium (10% FBS). Cholesterol and CD solutions were stored at 4ºC. A insertion complex of cholesterol:CD solution was prepared by dissolving 1mM cholesterol in ethanol, releasing into a glass test tube. The glass tube was then placed under nitrogen evaporation. 10mM CD was added to the glass test tube and vortexed. The glass test tube was then sonicated in a hot water bath for 3 min to detach cholesterol from the sides of tube. The cholesterol:CD complex solution was placed in a 37ºC

incubator upon a rocker overnight. Before application of treatment, a 0.45µM filter was used to filter the solution to take out cholesterol that did not go into solution. Solution was used immediately and never stored.

Morphometrics

N2a cells are plated into the 35mm cell culture dishes that contain a 1½ inch coverslip. Cells were plated at low densities (15,000cells/µl) and three dishes per treatment were performed. All 35mm dishes were incubated after plating without treatment. After 24h of incubation, all dishes were removed and placed under the phase contrast microscope to visualize cell confluence. For experiments, cells in 35mm dishes were treated at confluences between 30-40%. After application of treatment, dishes were incubated for an additional 24h. For differentiation observation, cell culture dishes are removed from the incubator and the coverslip was upended onto a glass microscope slide. The slide was then observed on a phase contrast microscope. Photomicrographs were taken on an Olympus BX51 microscope using Olympus BX60 Digital Camera and camera controlled software, DP controller. Photomicrographs of ten visual fields were taken at random from each treated and untreated (control) dish of cells.

Neurite Outgrowth Quantification

Cells that had one or more outgrowths that reached double the diameter of the cell body were considered to be differentiated. The differentiated cell percentage was determined by counting all cells in the ten photomicrographs from each treatment dish,

then counting the number of cells that were neurite bearing. The number of neurite bearing cells were divided by the number of cells counted to determine the percentage of differentiated cells.

Assessment of Acetylcholinesterase Activity

Cells were plated at 15,000cells/µl and grown in 100mm cell culture dishes in DMEM/ F-12 50/50 supplemented with 10% FBS, pen/strep and vitamins, in triplicate to 60-70% confluence. Cells were treated with appropriate reagent. After indicated treatment times (4, 8, 12, 24h), media was removed from the cell culture dishes. Cells were placed on ice and gently washed three times with chilled 1ml 0.05M Tris pH 7.4. After the third wash, 1ml of 0.05M Tris pH 7.4 was added and cells were scraped with a rubber policeman into 2ml microcentrifuge tubes. Cells were homogenized by performing 25 strokes with a tight pestle of a dounce homogenizer, while retaining homogenizer in an ice bucket. The cell homogenate was then released into a 2ml microcentrifuge tube that had been on ice and was then centrifuged at 12,000xg at 4°C for 10 min. The supernatant was removed from the 2ml microcentrifuge and released into a new 2ml microcentrifuge tube that had been in ice, the cell pellet was thrown away. The supernatant was vortexed and placed on ice. A Pierce BCA assay was used to determine the protein concentration of the supernatant of control and treated cells. Standards and unknown samples were loaded into a 96-well plate and incubated for 30 min at 37^0C in 5% CO_2 atmosphere. Following incubation, the plate was brought to room temperature, an OPTIMax Plate Reader using SoftMaxPro version 2.4.1 software

was used to quantify protein concentrations. Absorbance was measured at 562 nm. BCA

assay was performed to normalize protein concentrations for the acetylcholinesterase

(AChE) assay. To determine the AChE activity, a modified version of Ellman's

colorimetric assay was performed (Ellman 1961), using equal amounts of protein

between samples. Buffers used were 0.05M Tris pH 8.0 and 0.05M Tris pH 7.4.

Reagents included 4.04×10^{-3}M 5, 5-dithio (bis-2-nitrobenzoic acid) (DTNB) in 0.05M

Tris buffer pH 7.4 and 8.33×10^{-3} acetylthiocholine iodide salt (AThCh) in milliQ water.

The DTNB reagent is used to measure the amount of sulfhydryl groups in each sample

while AThCh is a substrate used in restoring the natural substrate acetylcholine.

Excluding 0.05M Tris pH 8.0, all reagents, buffers and samples were kept on ice during

preparation of the AChE assay. OPTIMax Plate Reader using SoftMaxPro version 2.4.1

software was used to measure AChE activity with absorbance at 412nm.

Western Blot Analysis

Cells are plated at 15,000 cells/µl and grown in 100 mm cell culture dishes

containing DMEM/ F-12 50/50 supplemented with 10% FBS, pen/strep and vitamins to

60-70% confluence. Dishes were grown in triplicate, treated appropriately, and harvested

at time intervals of 4, 8, 12, and 24 hours. After treatment times had ceased, culture

media was removed. The cells were placed on ice and then washed three times with 1ml

of chilled phosphate buffer saline (PBS). After the third wash, 1ml of chilled PBS was

used to harvest cells. Cells are scraped with a rubber policeman into a 2ml

microcentrifuge tube. Lysis buffer was added to the sample tubes and a 20 g 1½ needle

was used to pass the cells through three times to homogenize the cells. The samples are then placed in a centrifuge, spun at 12,000xg at 4˚C for 5 minutes. The supernatant was removed 2ml microcentrifuge and the cell pellet was discarded. The samples protein concentrations were determined by a Pierce BCA Assay Kit. Standards and samples were loaded into a 96-well plate and incubated for 30 minutes at 37^0C and 5% CO_2. Following incubation, the plate was brought to room temperature and placed in OPTIMax Plate Reader using SoftMaxPro version 2.4.1 software, absorbance measured at 562 nm. Each sample was prepared in 2ml microcentrifuge tube comprising 75µg of protein diluted in loading buffer (2X, 3X, or 4X). 2% of 100% BME (Beta-mercaptoethanol) was added to the 2ml centrifuge tubes. The 2ml microcentrifuge tubes were closed; the lids were perforated with a needle then boiled for 5 min. After 5 min had expired, tubes were placed in centrifuge for 3 min to remove any residue that had accumulated on the sides of the tube. The molecular weight marker (18µl) and samples were then loaded into wells and separated on 7.5% polyacrylamide gel. Following electrophoresis, proteins were transferred at 4°C to PVDF membrane at 75 volts for 3h; the membrane was then blocked with 4% nonfat dry milk overnight at 4°C while on the orbital shaker. The PVDF membrane was then rinsed two times with 1X TBS-T for 5 min. PVDF was probed with primary antibody (1:1000) for AChE, NeuN, or MAPK in Kapak "seal-a-meal" bag for 90 minutes on the orbital shaker at room temperature. Primary and secondary antibodies were diluted in 1% non-fat milk in 1X TBS-T. After 90 min, PVDF was washed three times, 15 min per wash, in 1X TBS-T while on the orbital shaker. The

PVDF was then probed with secondary antibody-HRP conjugate (1:10000) in Kapak "seal-a-meal" bag for 90 min on the orbital shaker at room temperature. The PVDF was rinsed 3 times, 10 min per wash, in 1X TBS-T with orbital shaking. The blots are prepared for visualization using western enhanced chemiluminescence, emmersed for 1 min. For Westerns blots involving co-treatment of mevinolin with mevalonolactone, FPP, and GGPP, were developed by placing blot in X-ray cassette and enveloped with X-ray film. Film was Blue Basic Autorad Film 5x7. Film was developed using an automated developer. Film required multiple exposures for best visualization. Blots for mevinolin co-treatment with GGPP (NeuN) and cholesterol, cholesterol:CD complex, and CD were visualized on a ChemiDoc MP system that allows high resolution and high sensitivity technology using by Image Lab 4.0 software.

RESULTS

The effect of treatment with the statin mevinolin on N2a cell differentiation

The experimental model for observing cell differentiation was the murine N2a neuroblastoma cell. For experiments, add-back treatments were performed to determine if intermediates of the pathway contribute to blocking or triggering cell differentiation. Experiments on N2a cells focused on treatments of the control, the inhibitor (mevinolin), the intermediate, and co-treatment of the inhibitor and intermediate. An independent intermediate alone was a control to establish if the intermediate blocks or triggers cell differentiation. Morphological examination of neurite outgrowth, the up-regulation of neuron specific enzymatic activity and the expression of neuronal specific proteins were measured in all add-back experiments. For cells to be deemed differentiated they must have increased activity in each of the differentiation determinants. These three determinants were used in defining a differentiated cell. The neuronal specific proteins and enzymes that are observed at minimal levels or are non-existent in undifferentiated cells will be amplified in the differentiated cell due to neuroblastoma cells deriving from sympathetic post-synaptic neurons. Acetylcholinesterase (AChE) enzyme activity was tested as a marker of neuronal cell terminal differentiation. AChE is an enzyme found in post synaptic neurons as a hydrolyzing enzyme of the pre-synaptic neuron neurotransmitter, acetylcholine, at the neuromuscular junction (Koenigsberger 1997). Neuronal specific proteins, AChE and neuronal nuclei (NeuN), were measured in both control and treated cells. Neuronal differentiation is associated with the up-regulation of

AChE (Paraoanu 2008), while NeuN recognizes an unidentified, but nuclear specific protein (Sarnat 1998). Recent studies have finally recognized the nuclear specific protein NeuN as Fox-3. Fox-3 is only expressed in neuronal tissues and is a member of the Fox-1 gene family. Fox-3 functions as a splicing factor, mediating pre-mRNA splicing (Kim 2009).

Neuroblastoma (N2a) cells were grown in cell culture medium (DMEM/F-12) containing 10% FBS, pen/strep and vitamins. Untreated N2a cells proliferated and displayed a round cellular morphology, smooth plasma membrane, nucleus located in the epicenter of the cell, and scarce cytoplasm. The vast majority of these N2a cells displayed an undifferentiated cell morphology. For cells to be considered differentiated, cells must project neurite outgrowths that extended double the diameter of the cell body. A small percentage of cells underwent spontaneous differentiation, <5%. To determine the role of the cholesterol synthesis pathway on cellular differentiation, HMG-CoA reductase was targeted by the statin drug, mevinolin. The aggressive blocking of HMG-CoA reductase by mevinolin averts the conversion of HMG-CoA into mevalonate. This aversion depletes the N2a cell of both sterol and non-sterol isoprenoids, inhibiting production of all downstream end products. By inhibiting the start of the pathway and adding back specific intermediates, we were able to clarify the intermediate that was involved in differentiation of the N2a cell.

To determine the concentration of mevinolin that resulted in optimum neurite outgrowth, a dose-response of mevinolin was determined to establish the concentration

that effectively induced optimum neurite outgrowths. Cells were plated and cultured until

30-40% confluency was reached; cells were then treated with concentrations of 5, 10, or

15 µM mevinolin. 24h post treatment cellular morphology was observed. Treated N2a

cells began to display an altered morphology typical of differentiation after treatment

with statins, as shown in previously published results (Maltese 1985, Evangelopolous

2009). Morphometric analysis provides that elimination of downstream intermediates by

mevinolin treatment induces neurite outgrowths, indicative of differentiation. Control

cells exhibited low amounts of spontaneous differentiation. N2a cells treated with 5µM

mevinolin produced neurites at a 6% differentiation rate (Fig. 2B). Cells treated with

10µM mevinolin revealed 19.7% differentiation (Fig. 2C). N2a cells treated with 15µM

mevinolin only triggered a 13.2% differentiation (Fig. 2D). While our results are similar

to the literature, previous investigators got optimum differentiation with 25µM mevinolin

at 24h post-treatment (Maltese 1985), but in our experiments the optimal concentration of

mevinolin was 10µM. The higher concentration of mevinolin (15µM) did not correlate

with an increased amount of cellular differentiation, as shown in Table 1. Figure 3

presents a comparison of morphometric analysis between the mevinolin treatments.

After establishing that 10µM mevinolin produced the highest differentiation rate, a

time study was performed to determine the time, in a 24h span, that 10µM mevinolin was

most active in differentiating the neuroblastoma cells. Neurite outgrowths were produced

in a time dependent manner. As seen in Figure 4, 10µM mevinolin effectively induced

differentiation, with differentiation percentages increasing in subsequent hours post

treatment. Treated cells produced outgrowths at 2h post treatment and steadily increased into 12h. Differentiation percentages plateaued after 12h and then maxed out at the 20h interval. At the 18h, 20h, and 24h, percentages of differentiated cells reached above 40% indicating that mevinolin is most active between 18-24h post treatments.

Effect of mevinolin removal on N2a cell differentiation

Dose response results determined that 10μM mevinolin was the optimal concentration to trigger differentiation, reaching maximum N2a cell differentiation at 24h post–treatment. Unpredicted results occurred upon the removal of 10μM mevinolin from the N2a cells. Removal of mevinolin after indicated times was performed by a culture medium exchange. Morphometric analysis showed that10μM mevinolin at 12h post-treatment produced 19% differentiation whereas 10μM mevinolin at 24h post-treatment triggered 29% differentiation rate. After the 12h and 24h time intervals had expired, a culture medium exchange occurred to wash away mevinolin from cells. Washes were observed at two time points during 12h treatment to 10μM mevinolin: 2h post 12h mevinolin treatment and 12h post 12h mevinolin treatment. The 2h post 12h treatment wash saw a swift blocking of differentiation, decreasing the differentiation rate to 4% differentiation and the 12h post 12h treatment saw the differentiation rate decrease to 1.5% differentiation. Washes for the 24h treatment to 10μM mevinolin were viewed at two times: 2h post 24h mevinolin treatment and 24h post 24 mevinolin treatment. 2h post 24h mevinolin treatment wash saw a dramatic decrease in differentiation from 29% to 8%, observing the removal as blocking differentiation. 24h post 24h mevinolin

treatment saw the differentiation rate continue to decrease, reaching 2.1% differentiation. Washes, removing mevinolin treatment, produced cellular differentiation in accord with the control cells, as presented in Table 2. Comparison between mevinolin treatments and washes are shown in Figure 6.

Effect of mevalonate on N2a cell differentiation induced by mevinolin

Next, testing occurred to establish whether the participation of intermediates in cholesterol synthesis pathway induced or inhibited differentiation of N2a cells. Tests were intended to focus on the major intermediates that, themselves, produced other biologically active molecules. Add-back experiments of non-sterol and sterol intermediates (mevalonate, FPP, GGPP, and cholesterol) were performed to reveal where along the pathway the causative agent rests. Mevalonolactone (mevalonate in the form of a lactone) was the first intermediate to be added-back after the inhibition of the cholesterol synthesis pathway. Control cells maintained cancerous morphology, with a few cells displaying neurite extensions, indicating spontaneous differentiation. Cells treated with 10μM mevinolin produced a 27% differentiation rate (Fig 7B). Mevalonolactone alone did not induce cellular differentiation (2.3%), with cells maintaining morphology as seen in control cells (Fig 7C). When N2a cells were co-treated with mevinolin and mevalonolactone (Fig 7D) cells did not display an increased differentiation rate (4%), as shown in Table 3. Differentiation percentages can be observed providing a comparison between the treatments, shown is Figure 8. These

results provide that mevalonate does not contribute to differentiation, but blocks neurite outgrowth.

Due to these cells undergoing morphological changes, an up-regulation of acetylcholinesterase (AChE) enzyme activity was tested. Cells were treated, and after indicated times, were harvested for AChE enzyme assay. In Figure 9, AChE enzyme activity was seen to increase in mevinolin treated at 4h, and a two-fold increase in AChE enzyme activity occurred between 12h and 24h in mevinolin treated cells. The co-treatment of 150μM mevlonolactone and 10μM mevinolin induced a dramatic decrease in AChE enzyme activity. Mevalonolactone alone treatment did not increase AChE enzyme activity, resembling the AChE enzyme activity levels of the control cells.

Testing whether mevalonate triggered differentiation, cell samples were subjected to Western Blot analysis to determine if an up-regulation of the neuron specific proteins, AChE and NeuN, occurred. As shown in Figure 10, membranes were probed with neuron specific proteins from cell samples treated with mevinolin, mevalonolactone, or mevinolin co-treatment with mevalonolactone and harvested after indicated times. Probing of cell samples indicates that control and treated cells express AChE. However, mevinolin treated cells brought about an increased activation of AChE at 12 and 24h post treatments, while the co-treatment of mevinolin with mevalonolactone produced declining expression of AChE in contrast to the mevinolin treated cells. In addition, stimulation of NeuN can be seen in mevinolin treated cells at 24h post treatment. Mevalonolactone alone treatment shows suppression of NeuN upon reaching 24h. Co-

treatment of mevinolin and mevalonolactone saw an increased presence from 4h to 24h post treatment.

Effect of FPP on N2a cell differentiation induced by mevinolin

Proceeding down the pathway, intermediate FPP was tested to verify its role in continuing or preventing differentiation. Morphological observations can be seen in Figure 11 while Table 4 provides cell counts from morphological observations. Control cells exhibit a few cells undergoing spontaneous differentiation. Mevinolin (10μM) treated cells produced an increased amount of differentiated cells (Fig. 11B). 10μM FPP was added to cells as a positive control, displaying a continued cancerous morphology, seen in Figure 11C. The addition of FPP treatment alone did not trigger cell differentiation. Cells were co-treated with mevinolin (10μM) and FPP (10μM). Mevinolin co-treatment with FPP blocked N2a cell differentiation, as shown in Figure 11D. Table 4 provides cell counts from morphological observations. Differentiation summations are shown in Figure 12. AChE enzyme activity levels in10μM mevinolin, 24 h post-treatment, continued to produce the highest levels of AChE enzyme activity, as shown in Figure 13. Mevinolin co-treatment with FPP presented declined AChE enzyme activity levels and returned to that of the control cells. To further investigate the effects of co-treatment with mevinolin and FPP, cells were treated and harvested for antibody probing of neuron specific proteins, AChE and NeuN. Probing of cell samples indicates that control cells express low levels of AChE, while mevinolin shows increased expression of AChE, climaxing at 24h post treatment, shown in Figure 14. Mevinolin co-

treatment with FPP displayed diminished expression of AChE.   At 24h, mevinolin treated cells induced an up-regulation of AChE expression, while mevinolin co-treated with FPP showed diminishing expression 24h post treatment. FPP treatment alone did not influence AChE levels. NeuN expression in treated cells was greater than control cells. NeuN presence increased in 4h mevinolin treatment. NeuN appeared in mevinolin treated supplemented with FPP at 4-8h but levels lessened at 12h and 24h. FPP alone treatment expressed NeuN at levels similar to control cells.

Effect of GGPP on N2a cell differentiation induced by mevinolin

In the cholesterol synthesis pathway, GGPP was the next intermediate to be examined. Cancerous morphology is maintained in control cells, while some cells experienced differentiation, shown in Fig. 15. Cells treated with mevinolin (10μM) continued to induce typical differentiation (Fig. 15B). Cells were treated with 10μM GGPP and cells did not present neurite outgrowths (Fig. 15C). Co-treatment of GGPP and mevinolin caused a decrease in differentiation rate, to that of the control cells (Fig. 15D). Cell counts from morphological observations after treatments are shown in Table 5. Differentiation percentages can be seen in Figure 16. AChE enzyme activity steadily increased in the presence of mevinolin, beginning at 4h and peaking at 24h. Mevinolin co-treatment with GGPP saw AChE enzyme activity decrease considerably, reaching levels in comparison to the control cells. Cells treated only with GGPP did not up-regulate AChE enzyme activity, shown in Figure 17. The effects of treatments with GGPP were further tested to verify whether the intermediate triggered or blocked

differentiation.   Treated cell samples were subjected to Western Blot analysis to

determine if an up-regulation of neuron specific proteins, AChE and NeuN, resulted.

AChE was seen to be present in controls. When N2a cells were treated with 10μM

mevinolin, AChE levels upregulated in subsequent hours leading to the maximum level at

24h post treatment. GGPP co-treatment with mevinolin saw increased AChE levels

diminish from 4h to 24h, producing levels seen in control. NeuN was found in the

control cells and upregulated in the mevinolin treated cells. Decreased expression

occurred in the mevinolin co-treated with GGPP (Figure 18).

Effect of cholesterol on N2a cell differentiation induced by mevinolin

The final intermediate of the cholesterol synthesis pathway to be examined was

cholesterol. Cholesterol is required for membranogenesis (Siperstein 1984), as well as,

the advancement and successful completion of cell mitosis (Siperstein 1984, Fernandez

2004). The majority of cholesterol is located in the cellular membrane, as its purpose is to

maintain structure and regulate lipid fluidity (Ilangumaran 1998).   Due to cholesterol's

hydrophobic nature, it requires added assistance to cross the cell membrane. Cholesterol

was either dissolved in 95% ethanol or loaded into cholesterol vehicle, 2-hydroxypropyl-

β-cyclodextrin (CD). CD is a tube with a hydrophobic core that is presented as a "cage

for cholesterol" that can transport cholesterol across the cell membrane (Christian 1997).

In aqueous solutions, the CD core permits solubilizing of molecules that are generally

hydrophobic (Christian 1997). The control cells displayed low levels of differentiation,

shown in Fig. 19A. Mevinolin treatment continued to induce optimum differentiation,

generating a 19% differentiation rate (Fig. 19B). Mevinolin co-treatment with CD (0%

cholesterol), triggered few differentiated cells (5.4%), as shown in Figure 19C. The co-

treatment of mevinolin with CD showed decreased differentiation. The lab blamed CD as

the reason for the blocked cell differentiation, blocking mevinolin's actions. Next,

cholesterol dissolved in 95% ethanol was tested. Mevinolin co-treated with cholesterol

dissolved in 95% ethanol produced neurite outgrowths, displaying an increased

differentiation rate (14%), nearing levels produced by mevinolin (Fig. 19D). N2a cells

co-treated with mevinolin and cholesterol:CD complex blocked differentiation (6%),

shown in Figure 19E. These results are questionable due to CD affecting mevinolin's

actions in the positive control co-treatment. After observing the blocking of mevinolin's

actions, the vehicle, CD, is no longer trusted. The positive controls (not shown) did not

produce differentiated N2a cells. Morphometric analysis of the treatments with the

values deriving from three treatment dishes as shown in Table 6. Differentiation

percentage comparisons between treatments are displayed in Figure 20.

Testing of cholesterol's influence in N2a cell differentiation continued, by

measurement of AChE enzyme activity. AChE enzyme activity increased at 4h

mevinolin and steadily increased into 24h, in comparison to the control cells, and at 24h

mevinolin peaking in activity. Mevinolin co-treated with 2-hydroxypropyl-β

cyclodextrin (M+CD) did not have an increase in AChE enzyme activity but reversed the

effect of mevinolin blocking the up-regulation of the enzyme. Co-treating with

mevinolin and cholesterol dissolved in 95% ethanol (M+Et+Chol), saw the effects of

mevinolin blocked, preventing the up-regulation of AChE from 4h to 12h. Interestingly, at the M+Et+Chol 24h, AChE enzyme activity dramatically climaxed to 24h mevinolin levels. Reacting similarly was the mevinolin co-treated with cholesterol:CD complex (M+CD+Chol). AChE enzyme levels were low at 4h and 8h but increased at 12h then significantly increased at 24h as shown in Shown in Figure 21.

To determine if cholesterol triggered the expression of the neuron specific proteins, AChE and NeuN, cell samples were subjected to Western Blot analysis. All cell samples showed an increased expression of AChE, as shown in Figure 22. NeuN was observed in control cells and decreased expression occurred at mevinolin 4-24h post treatment. NeuN expression was increased in co-treated cells with the increased expression in cells co-treated with mevinolin and CD.
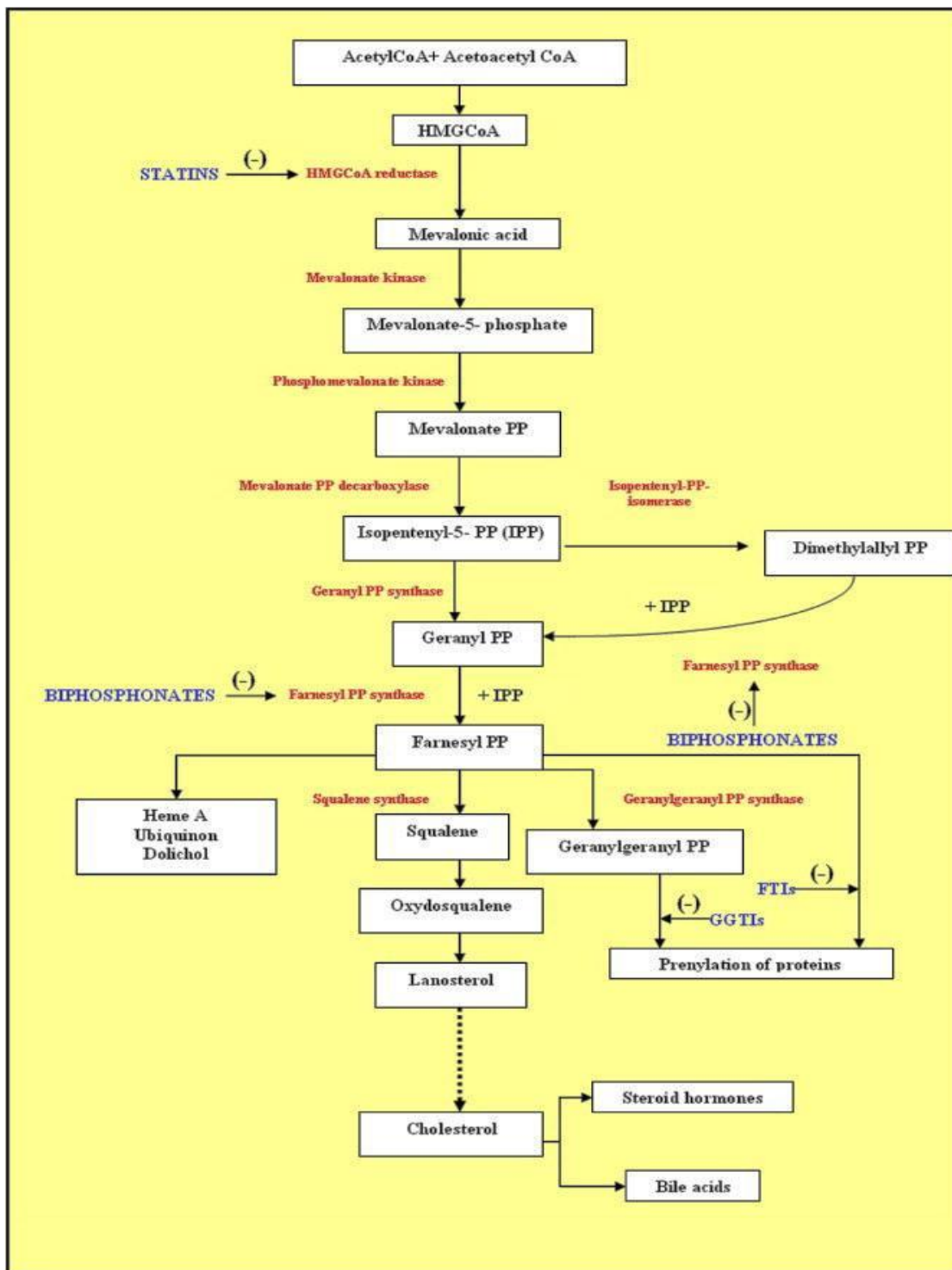
Figure 1. The Cholesterol Synthesis Pathway (Buhaescu 2007)
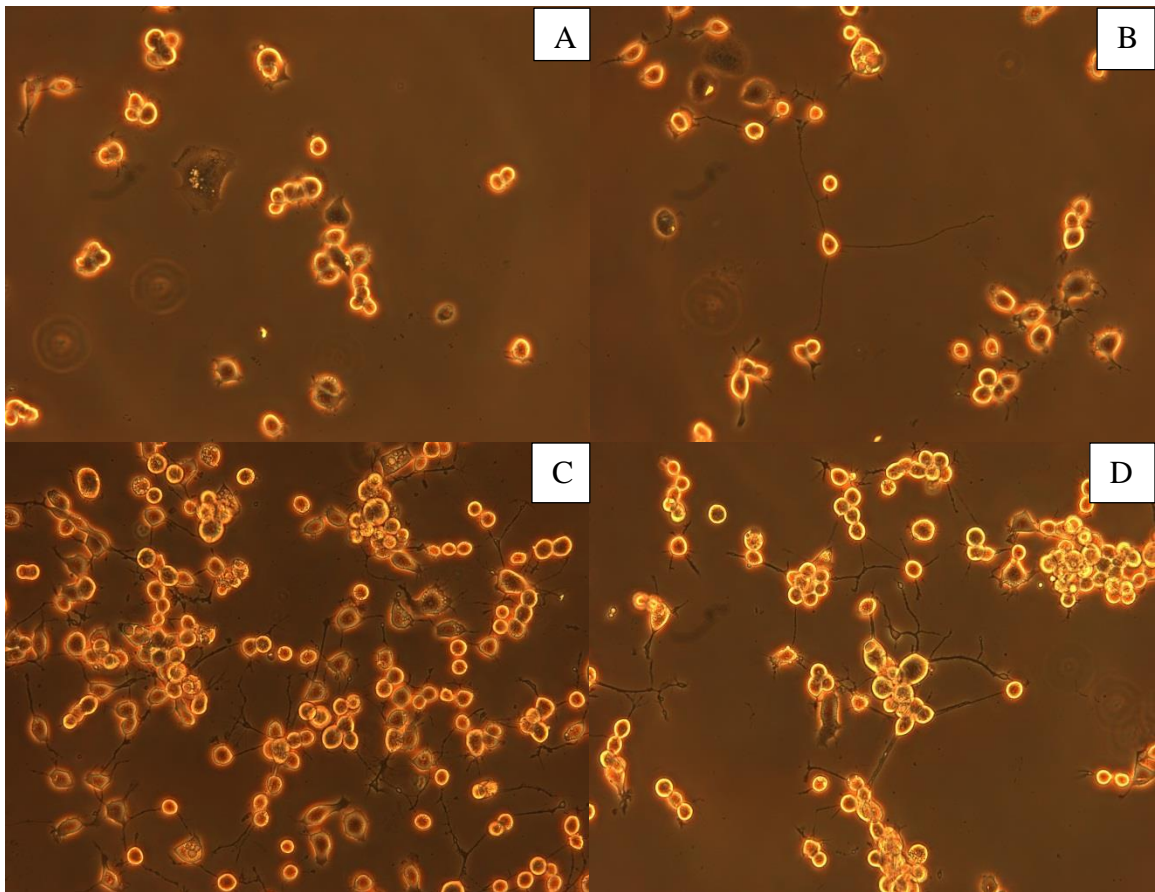
Figure 2. Morphological Observations of Mevinolin Dose Response. Cells were plated at 15,000 cells/µl in 35mm dishes containing culture medium and incubated. After reaching 30-40% confluence, treatments were added directly to culture medium and incubated. Treated N2a cells were photographed 24h post treatments for assessment of neurite extensions from dose response. Phase contrast microscopy was used to visualize cellular morphology. Photomicrographs were taken on an Olympus BX51 microscope using Olympus BX60 Digital Camera and camera controlled software, DP controller. A) Control N2a cells did not receive any treatment. B) N2a cells treated with 5µM mevinolin. C) N2a cells treated with 10µM mevinolin. D) N2a cells treated with 15µM mevinolin.

TABLE 1. Morphometric analysis of neurite outgrowth in mevinolin treated N2a cells

Cells were plated in 35mm dishes at 15,000 cells/µl, one dish for each treatment, and incubated. After reaching confluence of 30-40%, mevinolin treatments were administered directly to the culture medium. Cells either received no treatment (control), mevinolin (5µM), mevinolin (10µM), or mevinolin (15µM). At 24h post treatment, all treatments were viewed for measurement of neurite outgrowth. Coverslips were removed from dishes, placed on phase contrast microscope, and ten photomicrographs were taken. All cells in photomicrographs were counted and cells exhibiting neurites two times the length of the cell body were deemed differentiated. To establish the differentiation percentages, the numbers of differentiated cells were divided by the total number of cells. Values originated from each treatment dish.

Treatment	Cells	Differentiated Cells	Percentage of Differentiated Cells
Control	817	9	1.1
+Mevinolin (5µM)	511	30	5.9
+Mevinolin (10µM)	345	68	19.7
+Mevinolin (15µM)	515	68	13.2
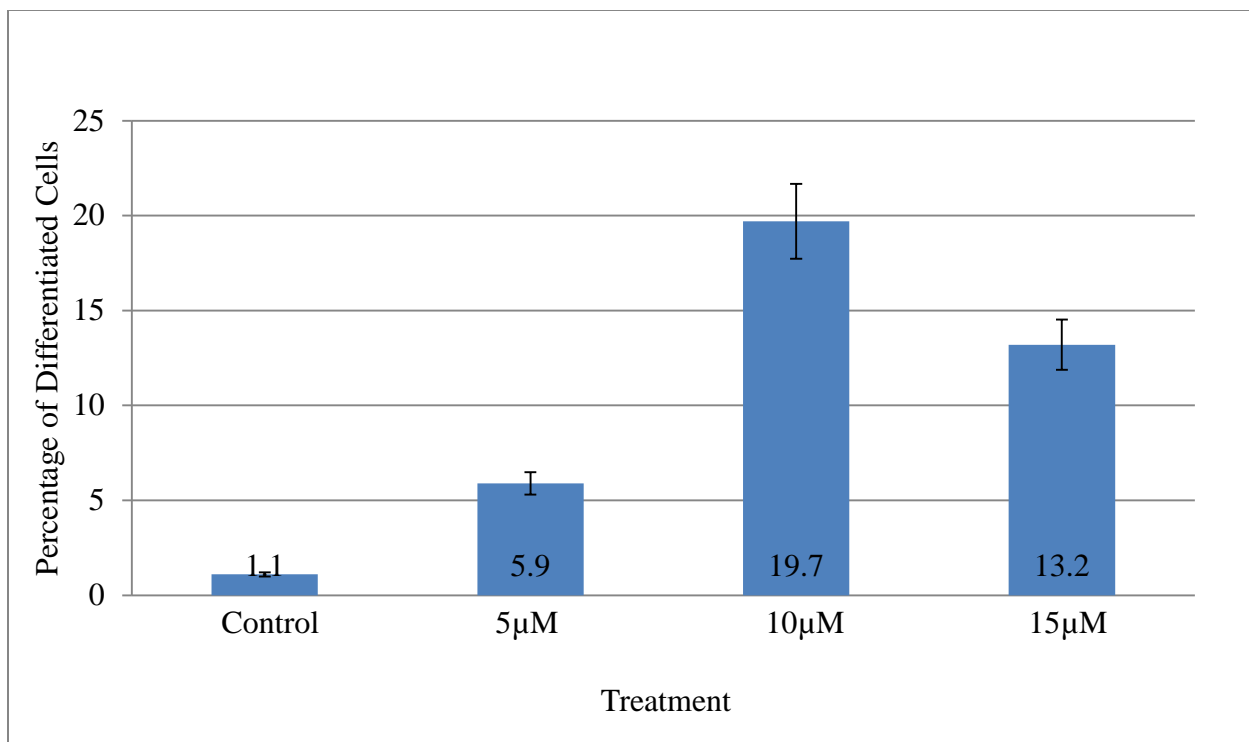
Figure 3. Differentiation summation of mevinolin dose response on N2a cells. N2a cells were plated at 15,000 cells/µl and grown in 35mm dishes, one per treatment, containing culture medium and were incubated. At 30-40% cell confluence, treatments (5, 10, 15 µM mevinolin) were administered directly to culture medium and dishes were incubated for additional 24h. Cells having neurite extensions measuring two times the length of the cell body were counted. Experiment was performed in triplicate. Percentages taken from TABLE 1.
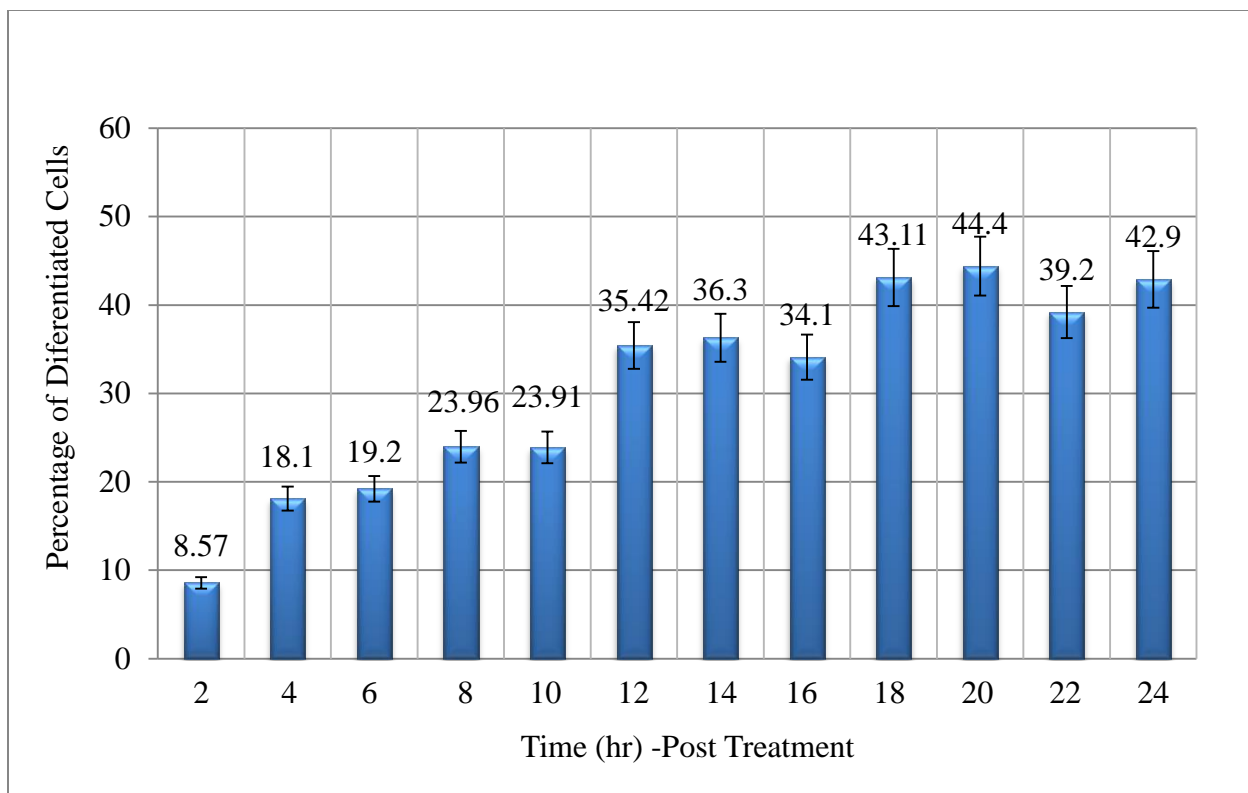
Figure 4. 24h time study of neurite outgrowth induced by mevinolin. N2a cells were plated at 15,000 cells/µl in 35mm dishes and incubated for 24h. All dishes received treatment of 10µM of mevinolin, added directly to the culture medium and incubated. Beginning 2h post treatment, cells were observed at 2h intervals, ending at 24h post treatment, under a phase contrast microscope where ten photomicrographs were taken, at random, of each dish to evaluate neurite outgrowth. All cells in photomicrographs were counted and cells with neurite outgrowths two times the length of the cell body were deemed differentiated. Differentiation percentages were established by dividing the neurite bearing cells by the total number of cells. Experiment was performed in duplicate.
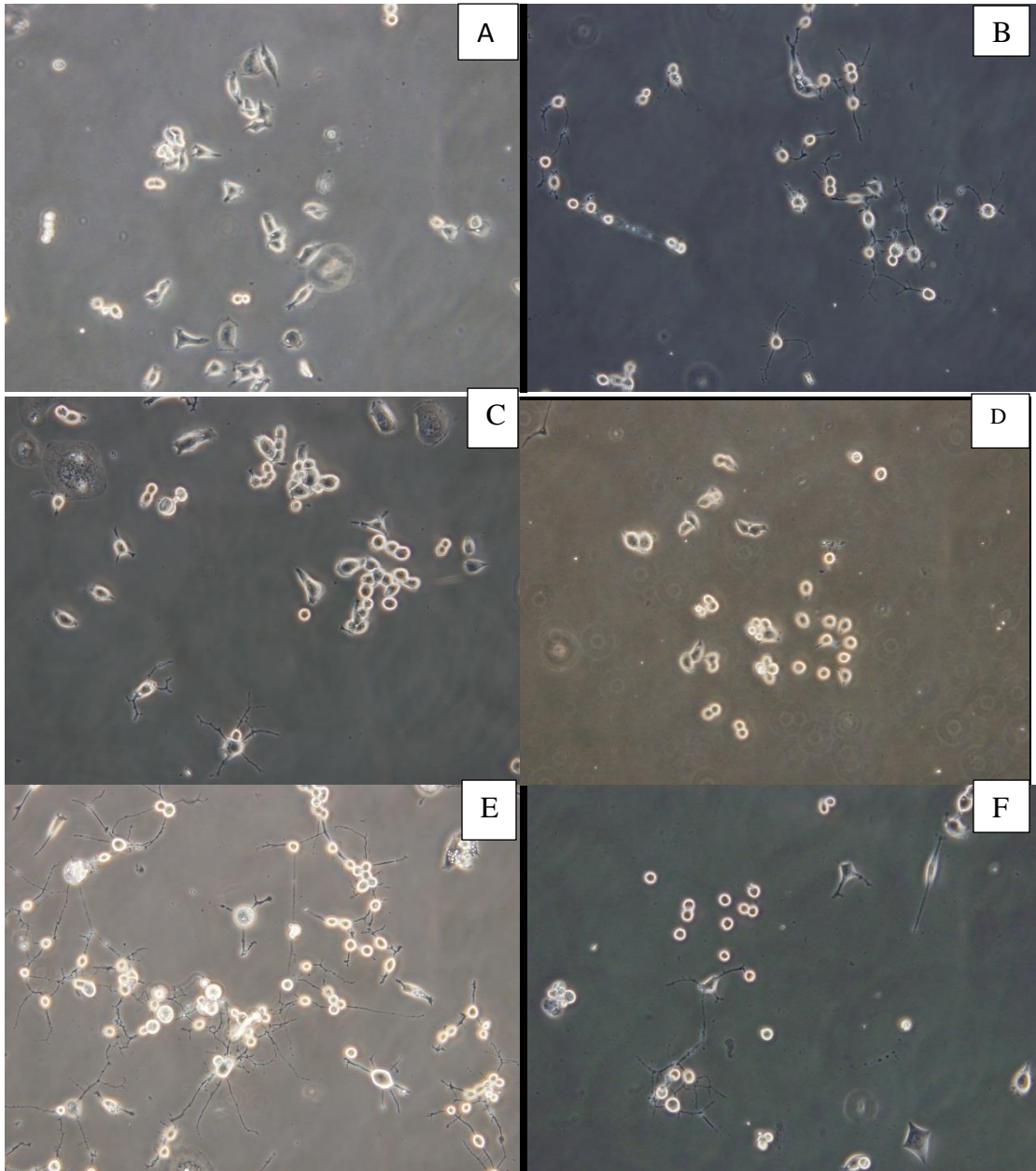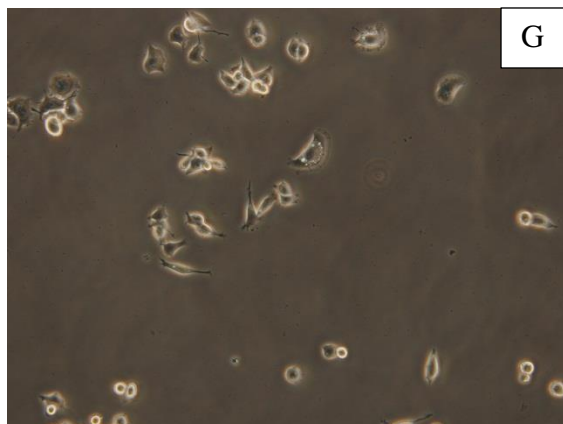
Figure 5. Morphological observations of mevinolin treatment and mevinolin removal on N2a cells. N2a cells were plated at 15,000 cells/µl in 35mm dishes and incubated for until cells reached 30-40% confluency. Treatments were added directly to culture medium and incubated. N2a cells were photographed after indicated times post treatment for assessment of neurites. Phase contrast microscopy was used to visualize cellular morphology. Photomicrographs were taken on an Olympus BX51 microscope using Olympus BX60 Digital Camera and camera controlled software, DP controller. A) Control N2a cells. B) Cells treated with 10 µM mevinolin for 12h. C) Cells treated with 10µM mevinolin for 12h, then received 2ml media wash for 2h. D) Cells treated with 10µM mevinolin for 12h, then received 2ml media wash for 12h. E) Cells treated with 10µM mevinolin for 24h. F) Cells treated with 10µM mevinolin for 24h, then received 2ml media wash for 2h. G) Cells treated with 10µM mevinolin for 24h, then received 2ml media wash for 24h.

TABLE 2. Morphometric analysis of mevinolin and mevinolin removal treated N2a cells

Cells were plated in 35mm dishes at 15,000 cells/µl, three dishes for each treatment, and incubated. After reaching confluence of 30-40%, treatments were administered directly to the culture medium. Cells either received no treatment (control), mevinolin (10µM). After treatment times, cells receiving a "wash" underwent a 2ml media exchange with culture medium.   At 24h post treatment, control, Mev12 and Mev24 were viewed for measurement of neurite outgrowth. Cells receiving "wash" were viewed at indicated times. Coverslips were removed from dishes, placed on phase contrast microscope, and ten photomicrographs were taken from each dish. All cells in photomicrographs were counted and cells exhibiting neurites two times the length of the cell body were deemed differentiated. To establish the differentiation percentages, the numbers of differentiated cells were divided by the total number of cells.

Treatment	Cells	Differentiated Cells	Percentage of Differentiated Cells
Control	1587	27	2.0
+Mev 12	928	175	19.0
+Mev12 2h post-wash	872	34	4.0
+Mev12 12h post-wash	320	5	1.5
+Mev24	1235	356	29.0
+Mev24 2h post-wash	691	54	8.0
+Mev24 24h post-wash	389	8	2.1
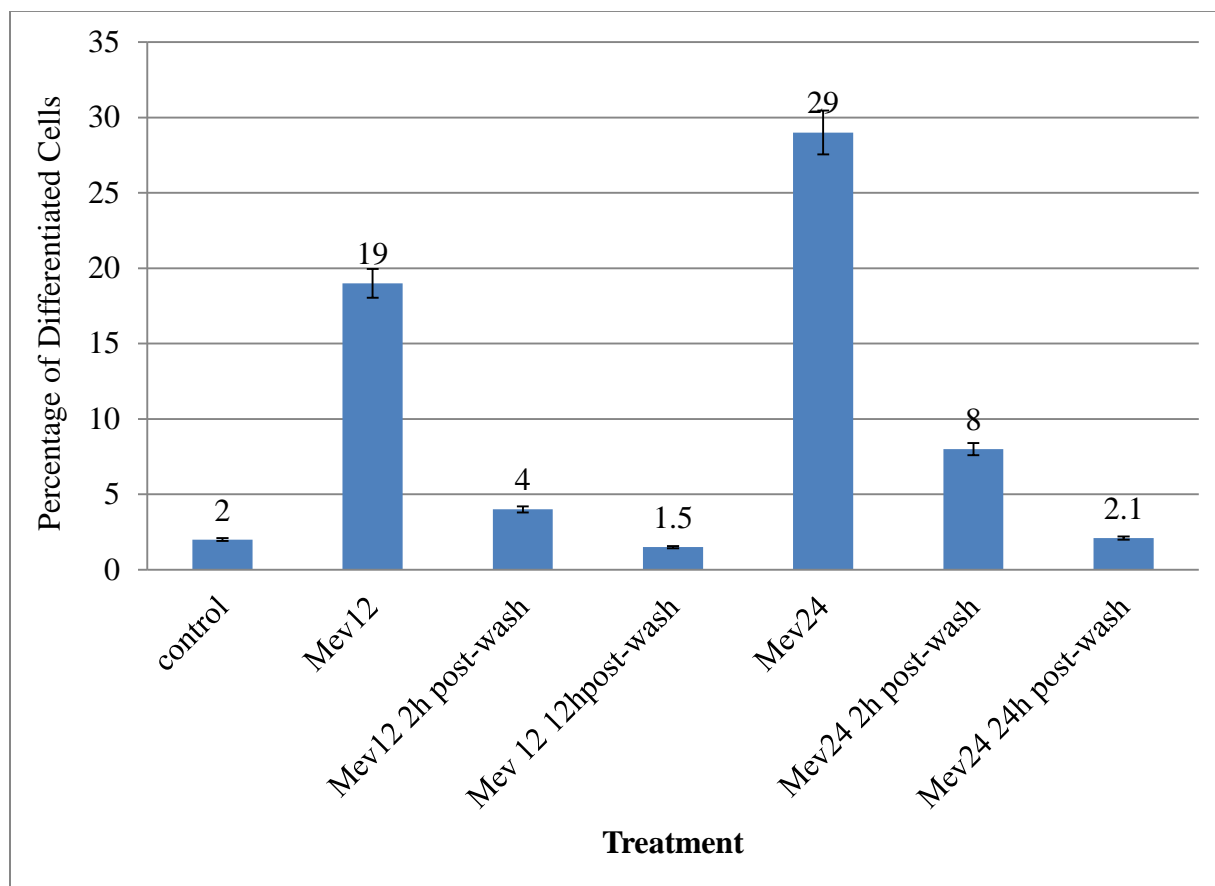
Figure 6. Differentiation summation of morphometric analysis of mevinolin treatment and mevinolin removal on differentiation of N2a cells. All cells in photomicrographs were counted and cells exhibiting neurites two times the length of the cell body were deemed differentiated. To reveal the differentiation percentages, the numbers of differentiated cells were divided by the total number of cells. Percentages were taken from TABLE 2. Mev= mevinolin.
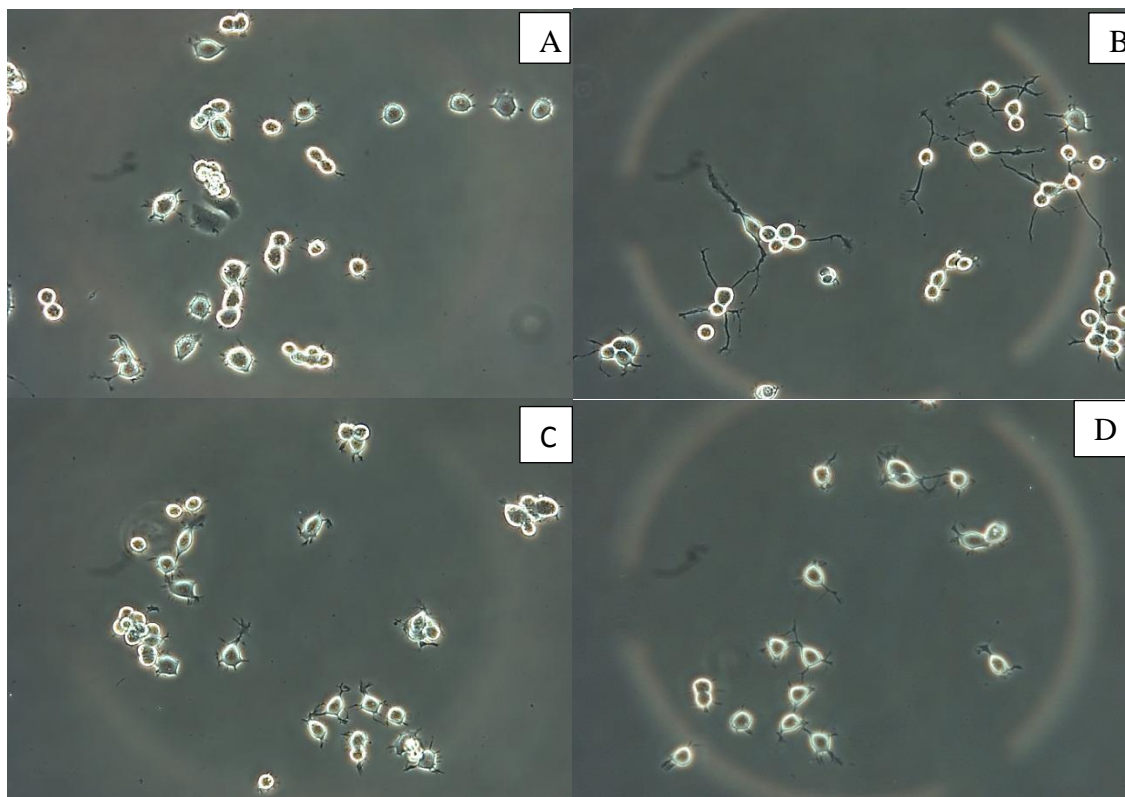
Figure 7. Morphological observations of mevinolin and mevalonolactone treated N2a cells. N2a cells were plated at 15,000 cells/µl in 35mm dishes and incubated for 24h. Treatments were added directly to culture medium and incubated. Treated N2a cells were photographed 24h post treatments for assessment of neurites. Phase contrast microscopy was used to visualize cellular morphology. Photomicrographs were taken on an Olympus BX51 microscope using Olympus BX60 Digital Camera and camera controlled software, DP controller. A) Control N2a cells did not receive any treatment. B) Cells treated with 10µM mevinolin. C) Cells treated with 150 µM mevalonolactone. D) Cells co-treated with 10µM mevinolin + 150µM mevalonolactone.

TABLE 3. Morphometric analysis of mevinolin and mevalonolactone treated N2a cells

Cells were plated in 35mm dishes at 15,000 cells/µl, three dishes for each treatment, and incubated. After reaching confluence of 30-40%, treatments were administered directly to the culture medium. Cells either received no treatment (control), mevinolin (10µM), mevalonolactone (150µM), or co-treatment of mevinolin (10µM) + mevalonolactone (150µM). At 24h post treatment, all treatments were viewed for measurement of neurite outgrowth. Coverslips were removed from dishes, placed on phase contrast microscope, and ten photomicrographs were taken from each dish. All cells in photomicrographs were counted and cells exhibiting neurites two times the length of the cell body were deemed differentiated. To establish the differentiation percentages, the numbers of differentiated cells were divided by the total number of cells. Values originated from the totals of the three treatment dishes.

Treatment	Cells	Differentiated Cells	Percentage of Differentiated Cells
Control	624	21	3.4
+Mevinolin	476	130	27
+Mevalonolactone	959	22	2.3
+Mevinolin + Mevalonolactone	705	29	4

Figure 8. Differentiation summation of morphometric analysis of mevinolin and mevalonolactone treated N2a cells. All cells in photomicrographs were counted and cells exhibiting neurites two times the length of the cell body were deemed differentiated. To reveal the differentiation percentages, the numbers of differentiated cells were divided by the total number of cells. Percentages taken from TABLE 2. Mev= mevinolin, MC= mevalonolactone, M+M= mevinolin + mevalonolactone.
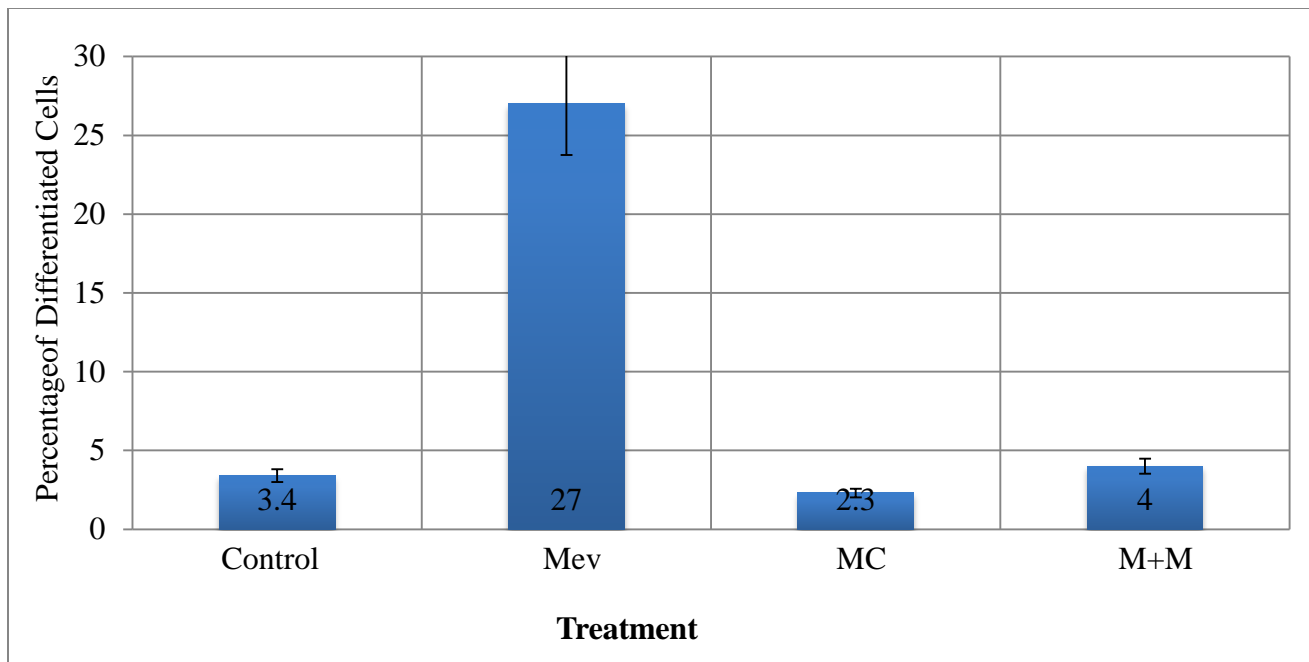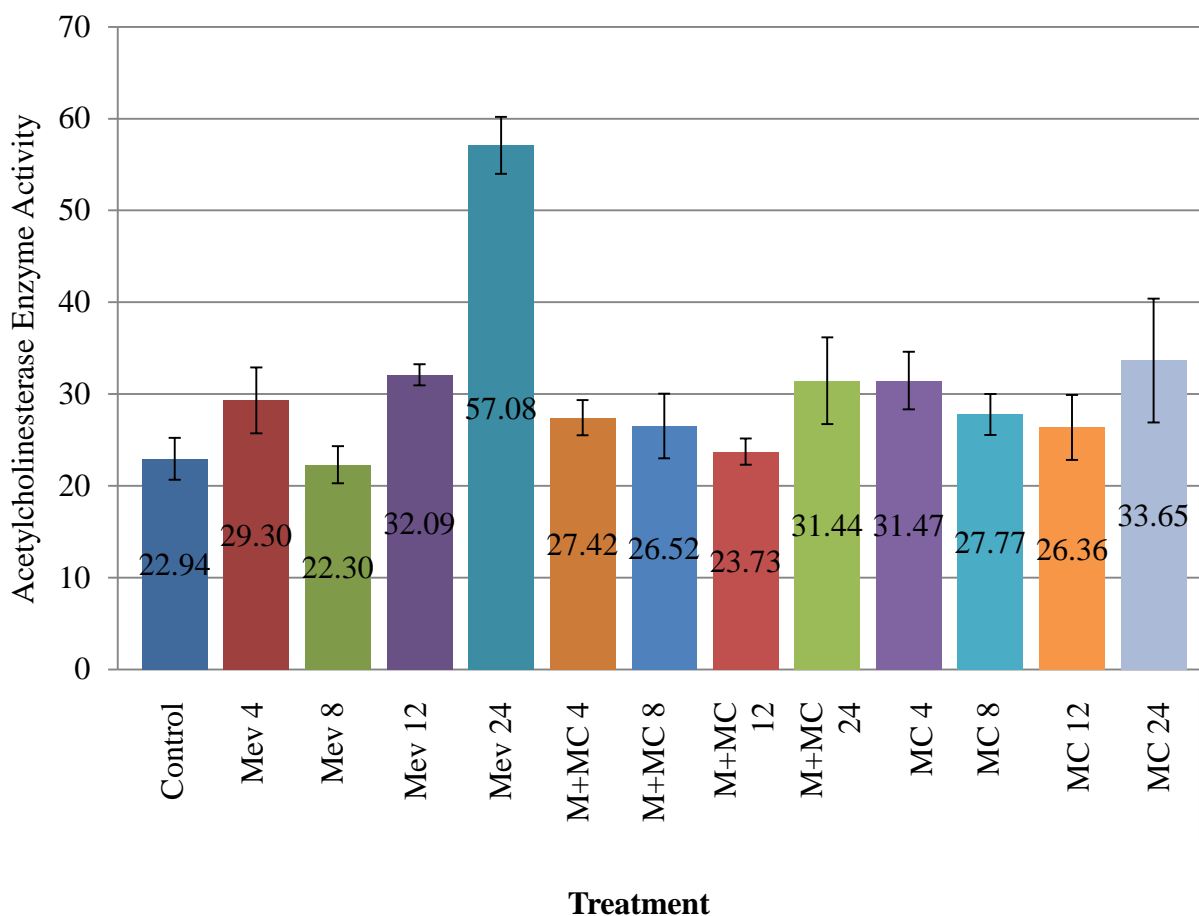
Figure 9. The impact of mevinolin and mevalonolactone on the acetylcholinesterase activity in N2a cells. Cells were plated and grown in 100mm dishes in culture medium and incubated. When cells had reached confluence, treatments were added directly to culture medium and incubated. Cells received treatments of 10μM mevinolin (M), 150μM mevalonolactone (MC), or co-treatment with 10μM mevinolin + 150μM mevalonolactone (M+M), and no treatment for control (C). After indicated times (shown in figure), cells were harvested in 0.05M Tris Buffer pH 7.4. Cells were homogenized using dounce homogenizer. A modified version of Ellman's assay was performed to determine acetylcholinesterase activity. Protein concentrations were normalized and loaded into 96-well plate along with 0.05M Tris pH 8.0, 4.04×10^{-3} M DTNB, and 8.33×10^{-3} M AThCh. OPTIMax Plate Reader using SoftMaxPro version 2.4.1 software was used to measure AChE activity. Absorbance was measured at 412nm.
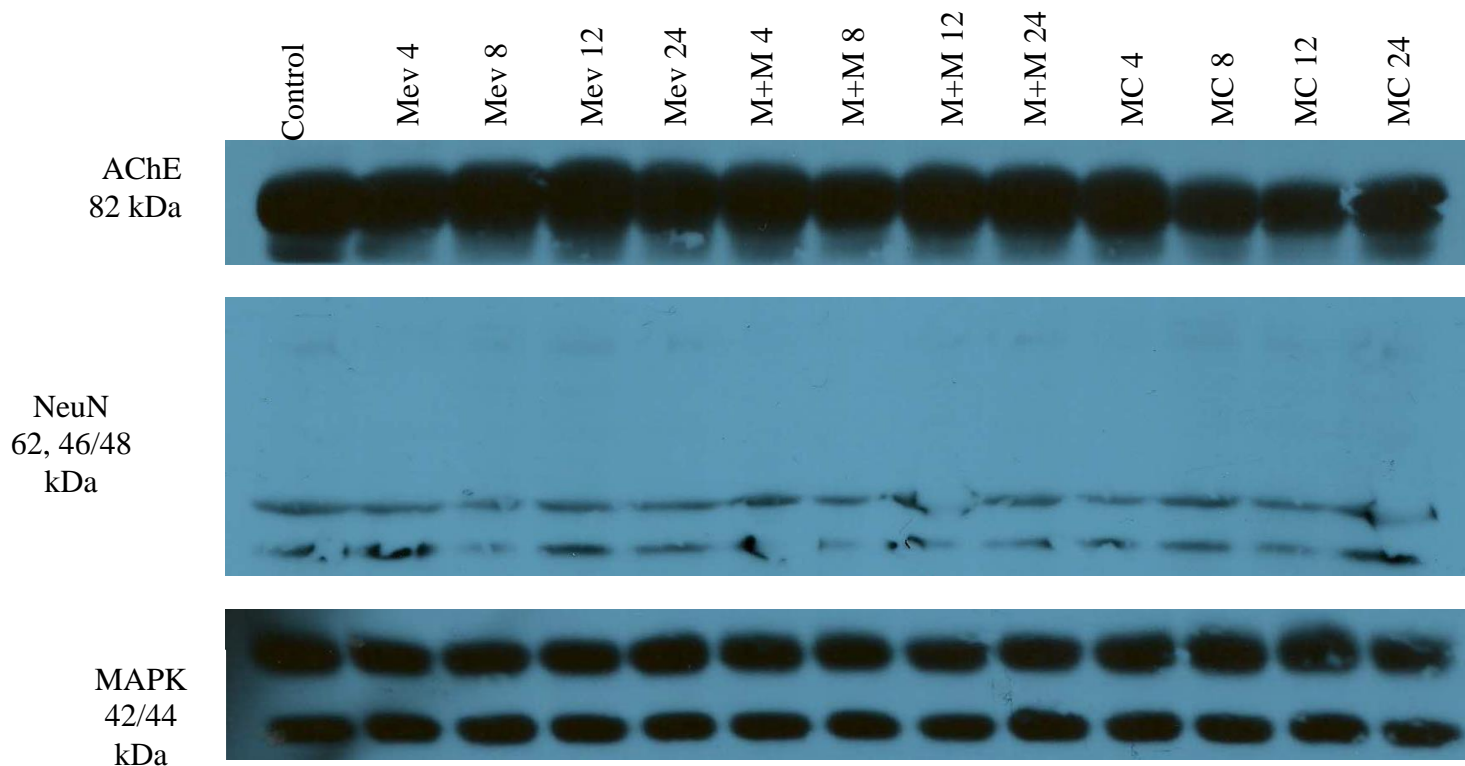
Figure 10. Neuron specific protein expression in N2a cells after administration of mevinolin and mevalonolactone. Cells were grown in 100mm dishes containing culture medium and incubated. When reaching appropriate cell confluence, treatments were administered directly to culture medium. N2a cells received no treatment (control), 10μM mevinolin (M), 150μM mevalonolactone (MC), or co-treatment of 10μM mevinolin+150μM mevalonolactone (M+M). After indicated times (shown above), treated cells were harvested, normalized by BCA assay, and 75μg of protein from each sample was separated by 7.5% SDS-PAGE, transferred to PVDF membrane and were western blotted for NeuN, AChE, and MAPK (loading control). To detect proteins, secondary antibodies were conjugated with horseradish peroxidase and visualized with enhanced chemiluminescence.
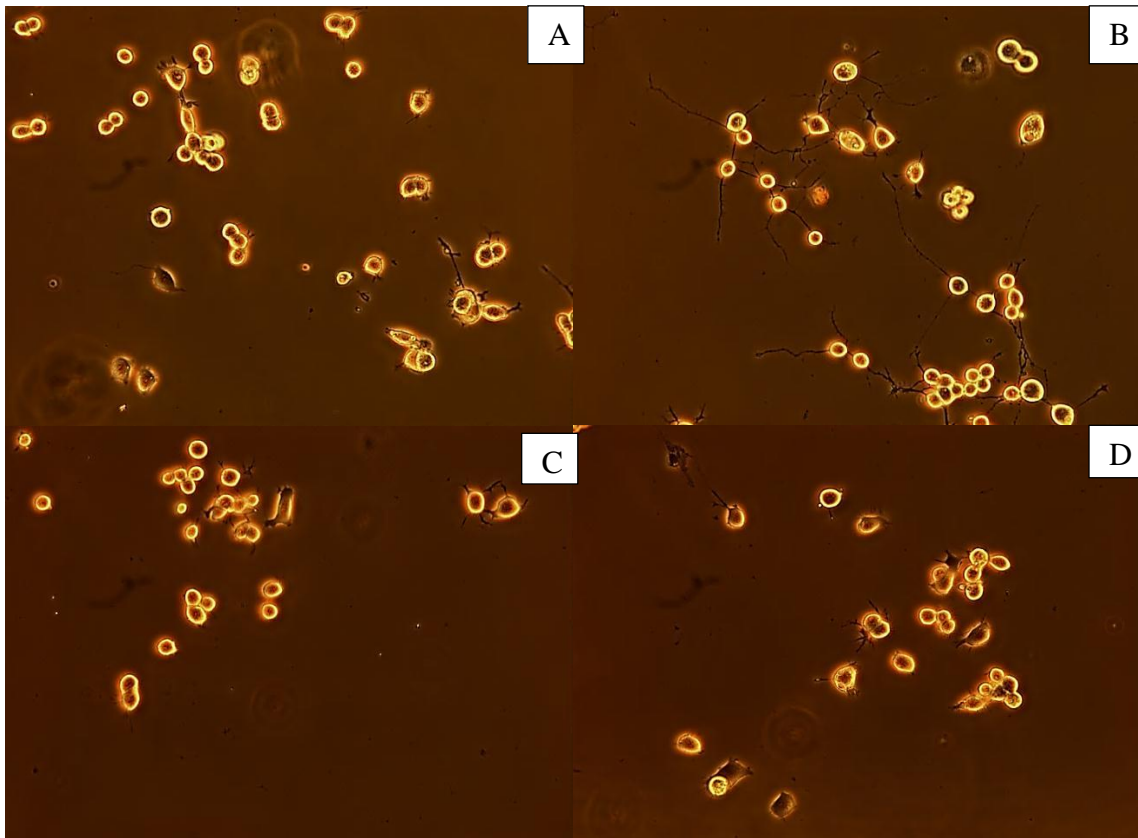
Figure 11. Morphological observations of mevinolin and farnesyl pyrophosphate treated N2a cells . N2a cells were plated at 15,000 cells/µl in 35mm dishes containing culture medium and incubated. Treatments were added directly to culture medium at 30-40% confluence and incubated. Treated N2a cells were photographed 24h post treatments for assessment of neurites. Phase contrast microscopy was used to visualize cellular morphology. Photomicrographs were taken on an Olympus BX51 microscope using Olympus BX60 Digital Camera and camera controlled software, DP controller. A) control dishes did not receive treatment. B) cells treated with 10µM mevinolin. C) cells treated with 10µM farnesyl pyrophosphate. D) cells co-treated with 10µM mevinolin + 10µM farnesyl pyrophosphate.

TABLE 4. Morphometric analysis of mevinolin and farnesyl pyrophosphate treated N2a cells

Cells were plated in 35mm dishes at 15,000 cells/µl, three dishes for each treatment, and incubated. After reaching confluence of 30-40%, treatments were administered directly to the culture medium. Cells either received no treatment (control), mevinolin (10µM), farnesyl pyrophosphate (10µM), or co-treatment of mevinolin (10µM) + farnesyl pyrophosphate (10µM). At 24h post treatment, all treatments were viewed for measurement of neurite outgrowth. Coverslips were removed from dishes, placed on phase contrast microscope, and ten photomicrographs were taken from each dish. All cells in photomicrographs were counted and cells exhibiting neurites two times the length of the cell body were deemed differentiated. To establish the differentiation percentages, the numbers of differentiated cells were divided by the total number of cells. Values originated from the totals of the three treatment dishes.

Treatment	Cells	Differentiated Cells	Percentage of Differentiated Cells
Control	1190	36	3.0
+Mevinolin	869	338	39
+Farnesyl Pyrophosphate	1236	16	1.3
+Mevinolin + Farnesyl Pyrophosphate	1074	64	6
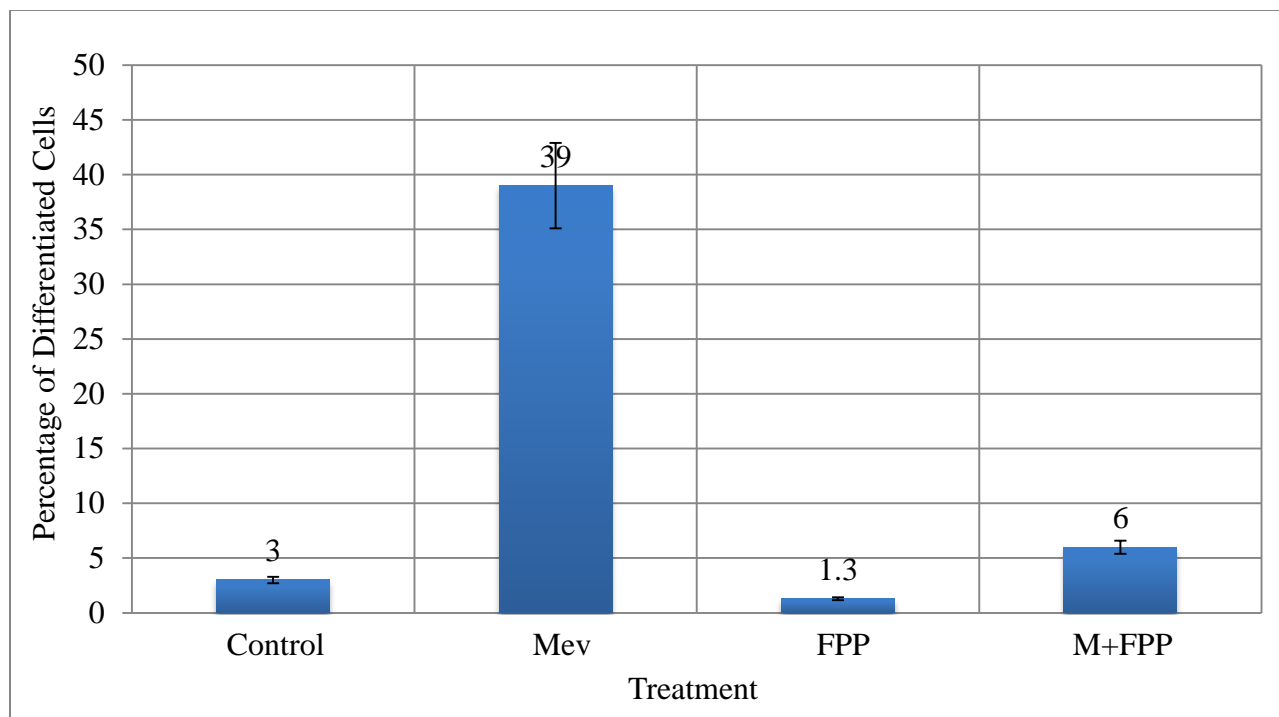
Figure 12. Differentiation summation of morphometric analysis of mevinolin and farnesyl pyrophosphate treated N2a cells. All cells in photomicrographs were counted and cells exhibiting neurites two times the length of the cell body were deemed differentiated and quantified. To reveal the differentiation percentages, the numbers of differentiated cells were divided by the total number of cells. Percentages are taken from TABLE 3. Mev= mevinolin, FPP= farnesyl pyrophosphate, and M+FPP= mevinolin + farnesyl pyrophosphate.
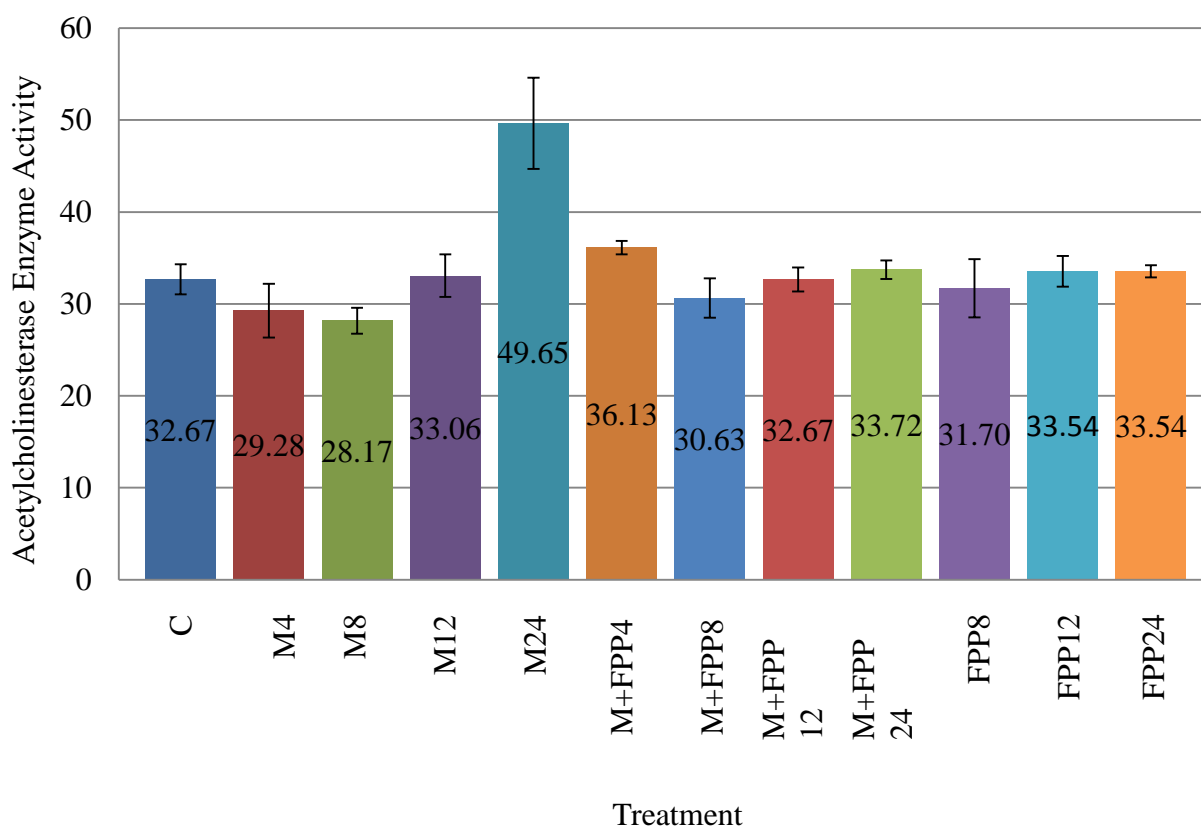
Figure 13. The impact of mevinolin and farnesyl pyrophosphate on the acetylcholinesterase activity. Cells were grown in 100mm dishes in culture medium and incubated. Treatments were added directly to culture medium and dishes were incubated. Treatments were added directly to culture medium and dishes were incubated. Cells received treatments of 10µM mevinolin (M), 10µM farnesyl pyrophosphate (FPP), or co-treatment of 10µM meviolin + 10µM farnesyl pyrophosphate (M+FPP). Controls (C) received no treatment. After indicated times shown in figure, cells were harvested in 0.05M Tris Buffer pH 7.4. Cells were homogenized using dounce homogenizer. Protein concentration of cells lysates were determined using Pierce BCA kit. A modified version of Ellman's assay was performed to determine acetylcholinesterase activity. Protein concentrations were normalized and loaded into 96-well plate along with 0.05M Tris pH 8.0, 4.04×10^{-3} M DTNB, and 8.33×10^{-3} M AThCh. OPTIMax Plate Reader using SoftMaxPro version 2.4.1 software was used to measure AChE activity. Absorbance was measured at 412nm. 4h FPP not shown.
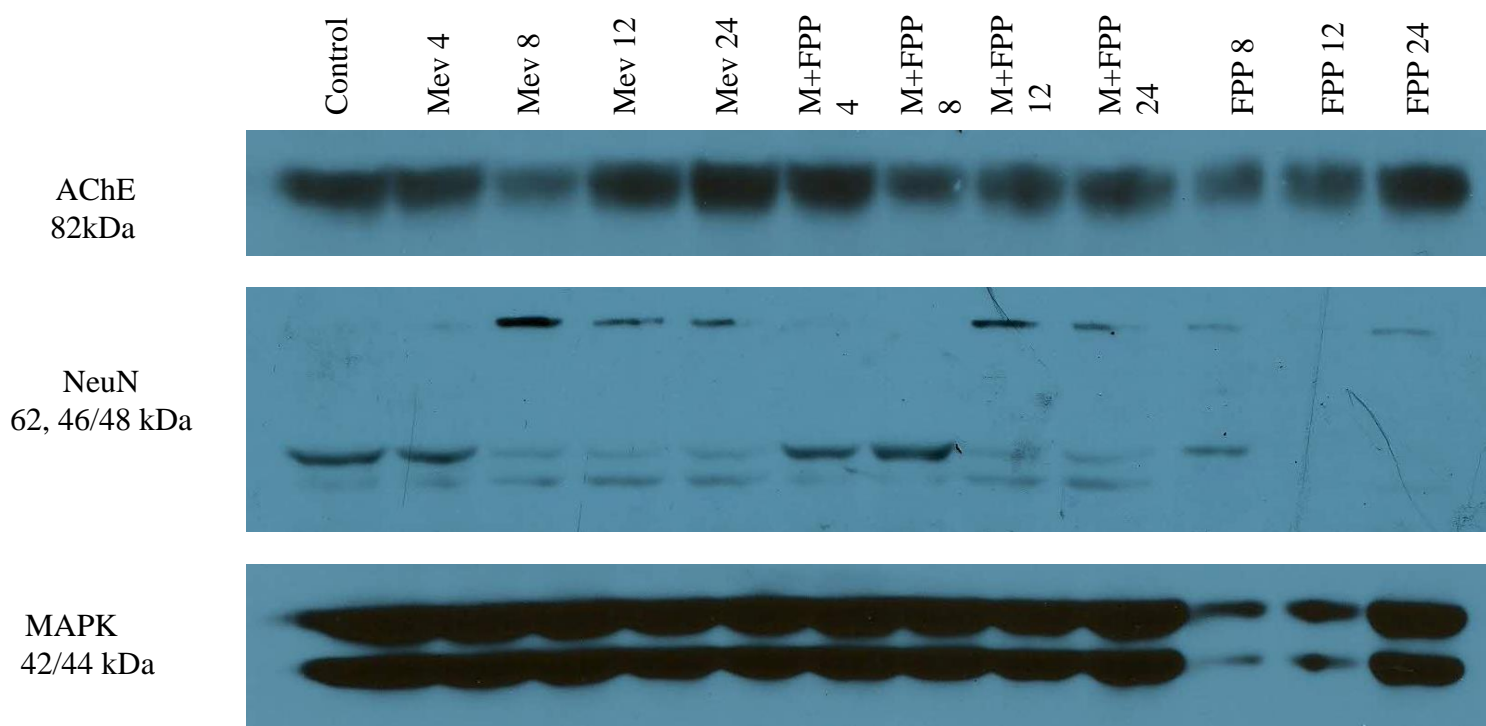
Figure 14. Neuron specific protein expression in N2a cells after administration of mevinolin and farnesyl pyrophosphate treatments. Cells were grown in 100mm dishes containing culture medium and incubated. When reaching appropriate cell confluence, treatments were administered directly to culture medium.   N2a cells received no treatment (control), 10μM mevinolin (M), 10μM farnesyl pyrophosphate (FPP), or co-treatment of 10μM mevinolin+10μM farnesyl pyrophosphate (M+FPP). After indicated times (shown above), treated cells were lysed, normalized by BCA assay, and 75μg of protein from each sample was separated by 7.5% SDS-PAGE, transferred to PVDF membrane and were western blotted for NeuN, AChE, and MAPK (loading control). To detect proteins, secondary antibodies were conjugated with horseradish peroxidase and visualized with enhanced chemiluminescence. 4h FPP not shown.
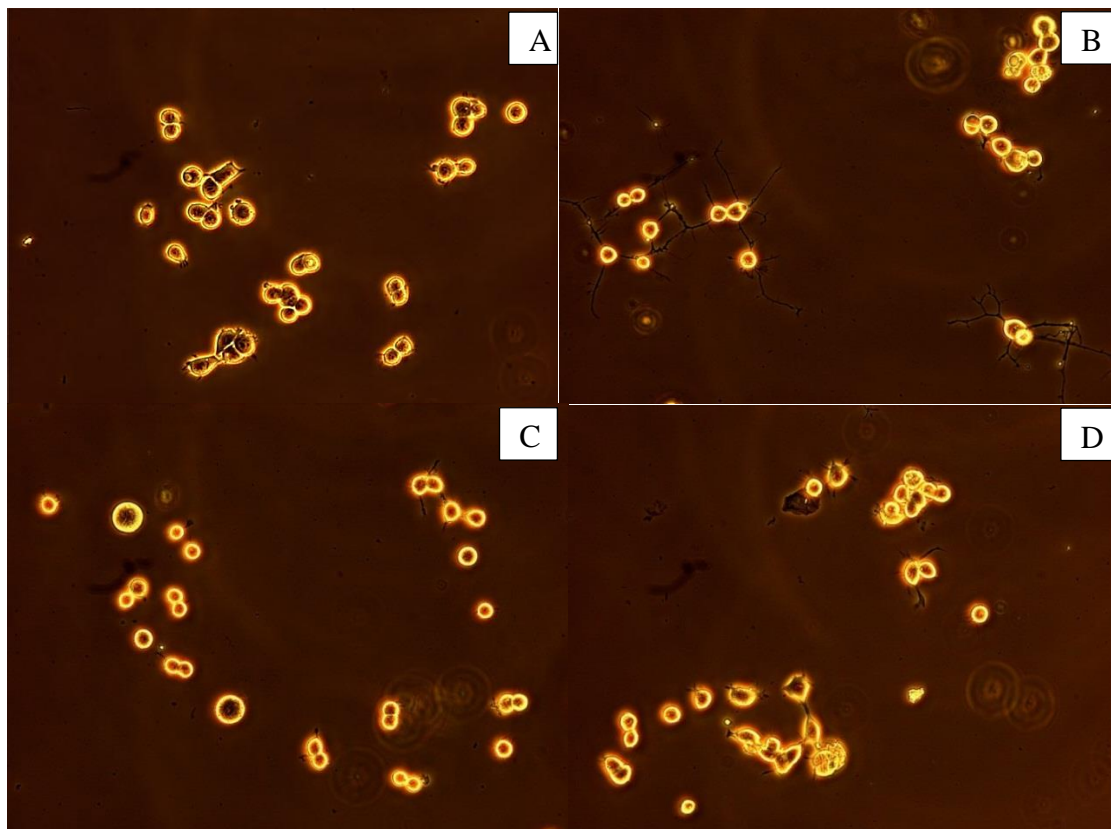
Figure 15. Morphological observations of mevinolin and geranylgeranyl pyrophosphate treated N2a cells. Cells were plated at 15,000 cells/µl in 35mm dishes containing culture medium and incubated. Treatments were added directly to culture medium at 30-40% confluence and incubated. Treated N2a cells were photographed 24h post treatment for assessment of neuritis extensions. Phase contrast microscopy was used to visualize cellular morphology. Photomicrographs were taken on an Olympus BX51 microscope using Olympus BX60 Digital Camera and camera controlled software, DP controller. A) Control dishes did not receive treatment. B) Cells received 10µM mevinolin. C) Cells received 10µM geranylgeranyl pyrophosphate. D) Cells received co-treatment of 10µM mevinolin + 10µM geranylgeranyl pyrophosphate.

TABLE 5. Morphometric analysis of mevinolin and geranylgeranyl pyrophosphate treated N2a cells

Cells were plated in 35mm dishes containing culture medium at 15,000 cells/µl, three dishes for each treatment, and incubated. After reaching confluence of 30-40%, treatments were administered directly to the culture medium. Cells either received no treatment (control), mevinolin (10µM), geranylgeranyl pyrophosphate (10µM), or co-treatment of mevinolin (10µM) + geranylgeranyl pyrophosphate (10µM). At 24h post treatment, all treatments were viewed for measurement of neurite extensions. Coverslips were removed from dishes, placed on phase contrast microscope, and ten photomicrographs were taken from each dish. All cells in photomicrographs were counted and cells exhibiting neurites two times the length of the cell body were deemed differentiated. To establish the differentiation percentages, the numbers of differentiated cells were divided by the total number of cells. Values originated from the totals of the three treatment dishes.

Treatment	Cells	Differentiated Cells	Percentage of Differentiated Cells
Control	777	11	1.4
+Mevinolin	622	154	25
+Geranylgeranyl Pyrophosphate	902	15	1.7
+Mevinolin + Geranylgeranyl Pyrophosphate	895	14	1.6
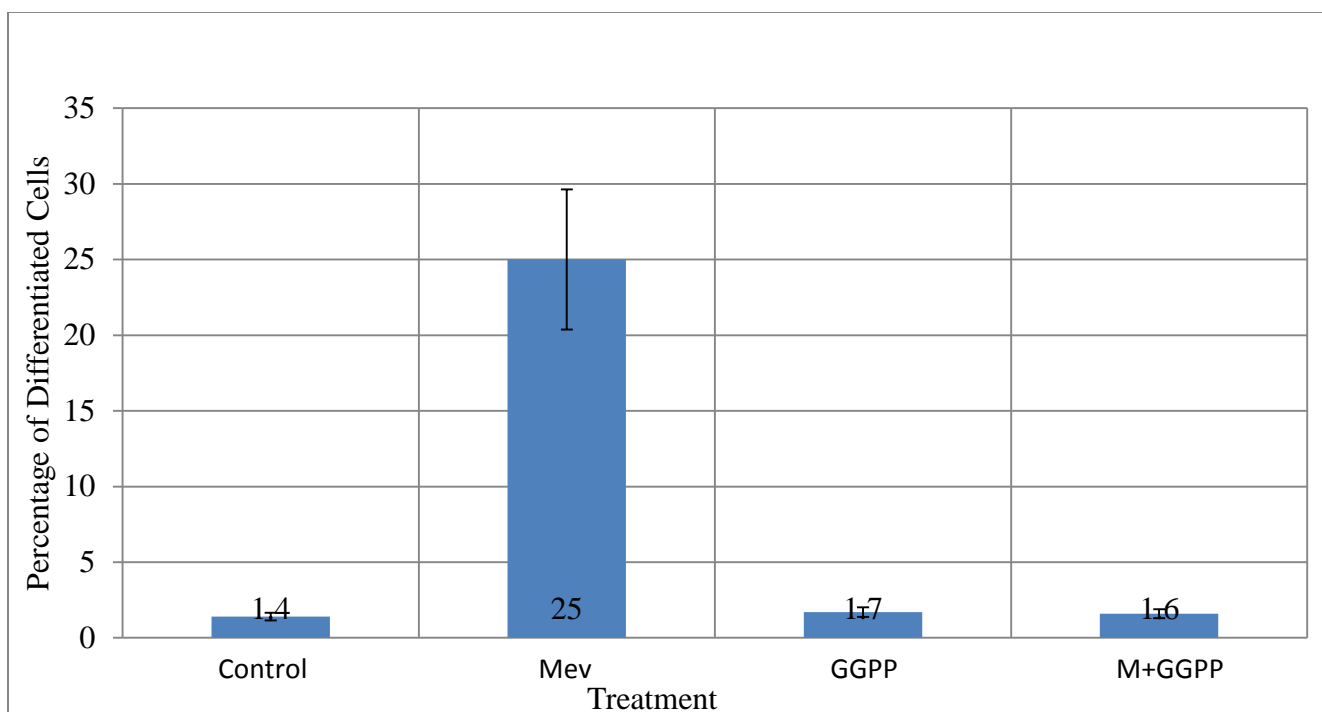
Figure 16.   **Differentiation summation of morphometric analysis of mevinolin and geranylgeranyl pyrophosphate treated N2a cells**. All cells in photomicrographs were counted and cells exhibiting neurites two times the length of the cell body were deemed differentiated. To reveal the differentiation percentages, the numbers of differentiated cells were divided by the total number of cells. Percentages were taken from TABLE 4. Mev= mevinolin, GGPP= geranylgeranyl pyrophosphate, M+GGPP= mevinolin + geranylgeranyl pyrophosphate.
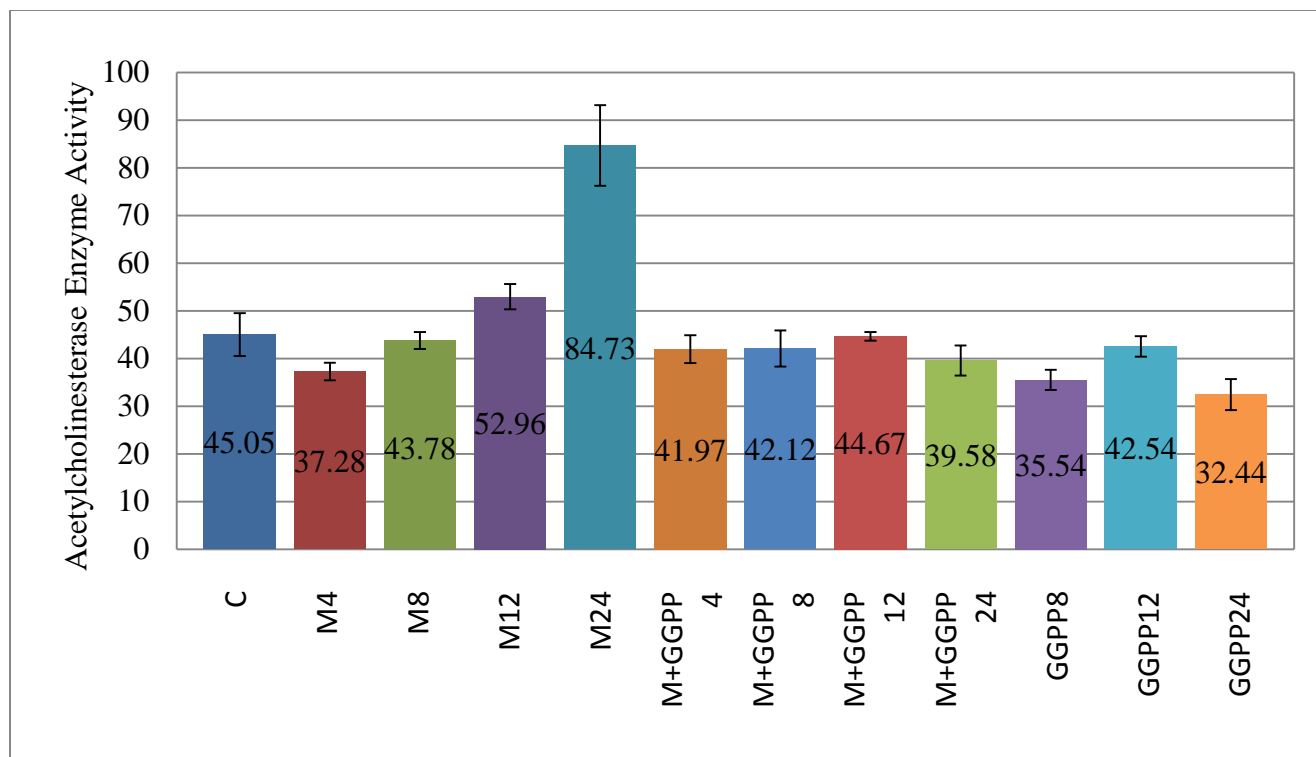
Figure 17. The impact of mevinolin and geranylgeranyl pyrophosphate on acetylcholinesterase activity. Cells were grown in 100mm dishes in culture medium and incubated. Treatments were added directly to culture medium and incubated. Cells received treatments of 10μM mevinolin (M), 10μM geranylgeranyl pyrophosphate (GGPP), or co-treatment of 10μM mevinolin + 10μM geranylgeranyl pyrophosphate (M+GGPP). Control (C) cells received no treatment. After indicated times shown in figure, cells were harvested in 0.05M Tris Buffer pH 7.4. Cells were homogenized using dounce homogenizer. Protein concentration of cells lysates were determined using Pierce BCA kit. A modified version of Ellman's assay was performed to determine acetylcholinesterase activity. Protein concentrations were normalized and loaded into 96-well plate along with 0.05M Tris pH 8.0, 4.04×10^{-3} M DTNB, and 8.33×10^{-3} M AThCh. OPTIMax Plate Reader using SoftMaxPro version 2.4.1 software was used to measure AChE activity. Absorbance was measured at 412nm. 4h GGPP not shown.
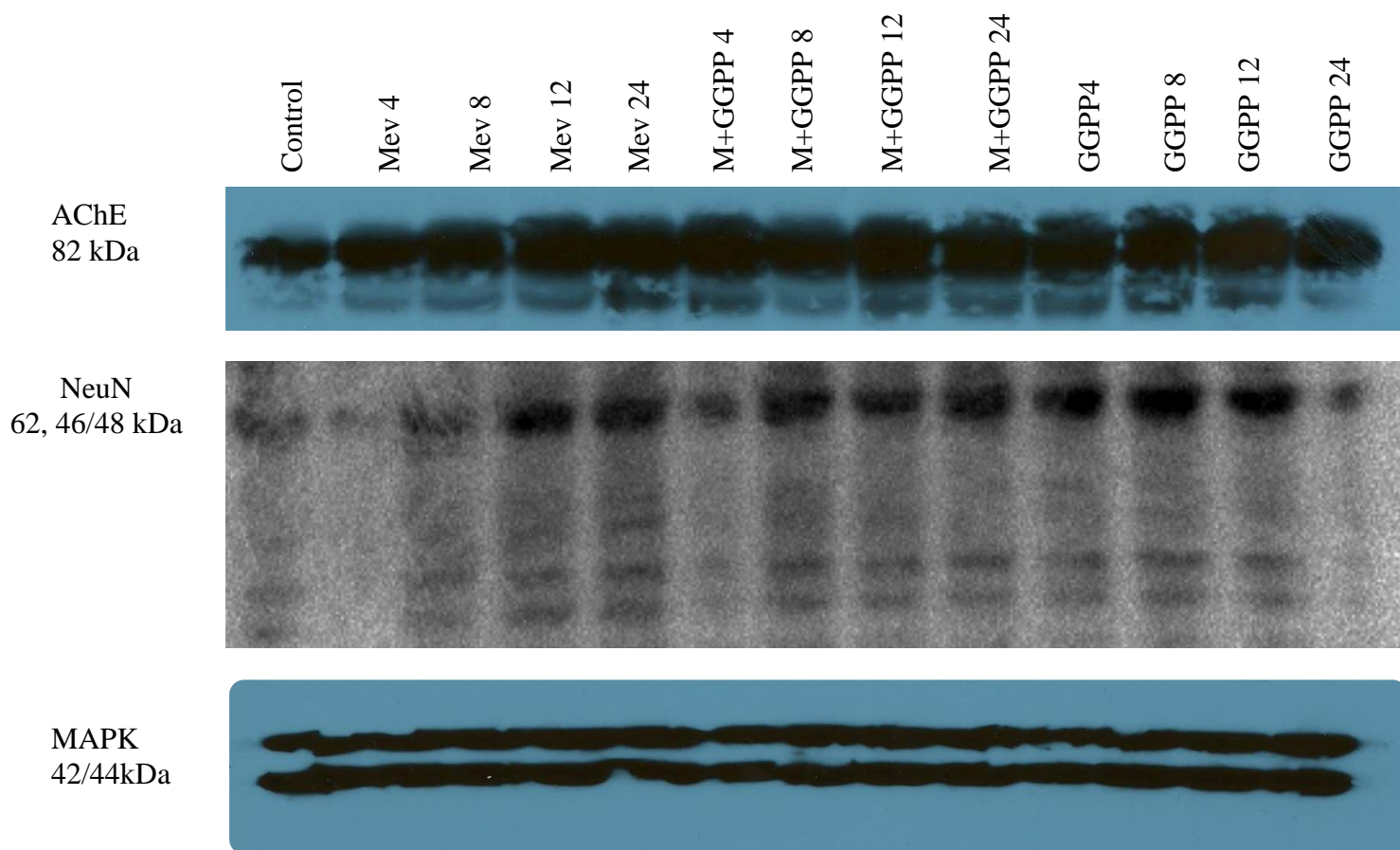
Figure 18. Protein expression in N2a cells after administration of mevinolin and geranylgeranyl pyrophosphate treatments. After indicated times (shown above) cell samples were lysed and 75µg of protein from each sample was separated by 7.5% SDS-PAGE, transferred to PVDF membrane and were western blotted for NeuN, AChE, and MAPK (loading control). To detect proteins, secondary antibodies were conjugated with horseradish peroxidase and visualized with enhanced chemiluminescence. C=control, M=mevinolin, GGPP=geranylgeranyl pyrophosphate, M+GGPP=mevinolin+geranylgeranyl pyrophosphate.
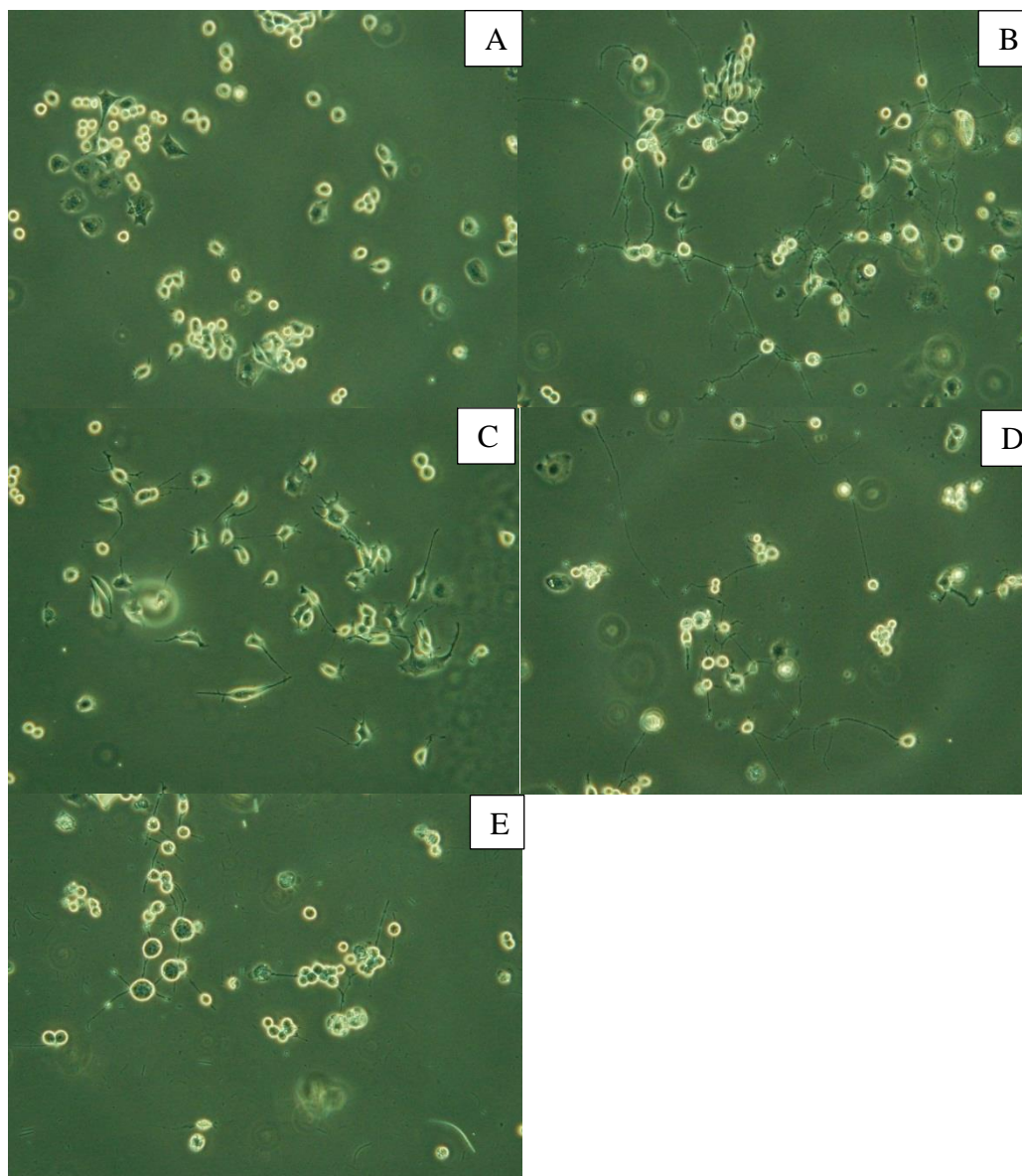
Figure 19. Morphological observations of mevinolin and mevinolin supplemented with 2-hydroxypropyl -β-cyclodextrin, cholesterol, or 2-hydroxypropyl-β-cyclodextrin loaded with cholesterol treated N2a cells. Cells were plated and incubated for 24h. Treated N2a cells were photographed 24h post treatments for assessment of neurites. Phase contrast microscopy was used to visualize cellular morphology. Photomicrographs were taken on an Olympus BX51 microscope using Olympus BX60 Digital Camera and camera controlled software, DP controller.   A) Control N2a cells did not receive any treatment. B) Cells treated with 10μM mevinolin. C) Cells with co-treatment of 10 μM mevinolin + 10mM 2-Hydroxypropyl -β-

cyclodextrin. D) Cells with co-treatment of 10μM mevinolin + 1mM cholesterol in ethanol. E) Cells with treatment of 10 μM mevinolin + 10mM 2-Hydroxypropyl -β-cyclodextrin loaded with 1mM cholesterol. Positive controls not shown.

TABLE 6. Morphometric analysis of mevinolin and mevinolin supplemented with 2-hydroxypropyl-β-cyclodextrin, cholesterol in ethanol, or 2-hydroxypropyl-β-cyclodextrin loaded with cholesterol treated cells

Cells were plated in 35mm dishes at 15,000 cells/μl, three dishes for each treatment, and incubated. After reaching confluence of 30-40%, mevinolin (10μM) and co-treatment of mevinolin (10μM) + (0.143mM) cholesterol in ethanol were administered directly to the culture medium. Mevinolin (10μM) + 2-hydroxypropyl-β-cyclodextrin (10mM) and mevinolin (10μM) + 2-hydroxypropyl-β-cyclodextrin (10mM) + cholesterol (1mM) treatments were performed as media exchanges. At 24h post treatment, all treatments were viewed for measurement of neurite outgrowth. Coverslips were removed from dishes, placed on phase contrast microscope, and ten photomicrographs were taken from each dish. All cells in photomicrographs were counted and cells exhibiting neurites two times the length of the cell body were deemed differentiated. To establish the differentiation percentages, the numbers of differentiated cells were divided by the total number of cells. Values originated from the totals of the three treatment dishes.

Treatments	Cells	Differentiated Cells	Percentage of Differentiation
Control	3077	20	0.0065
+Mevinolin	2109	407	19
+Mevinolin +2-Hydroxypropyl-β-cyclodextrin	2194	118	5.4
+Mevinolin +Cholesterol	2446	343	14
+Mevinolin +2-Hydroxypropyl-β-cyclodextrin +Cholesterol	1521	98	6
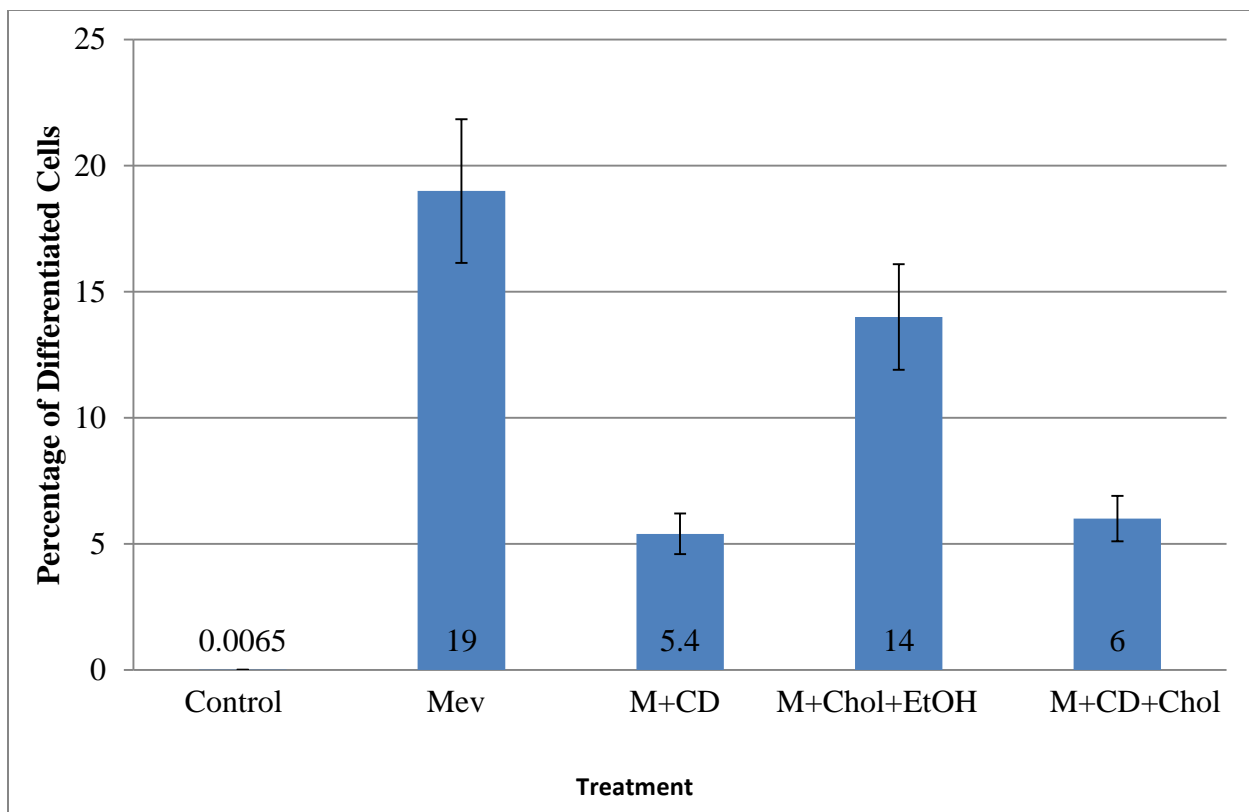
Figure 20. Differentiation summation of morphometric analysis of mevinolin and mevinolin supplemented with 2-hydroxypropyl -β-cyclodextrin, cholesterol, or 2-hydroxypropyl-β-cyclodextrin loaded with cholesterol treated N2a cells. All cells in photographs were counted and cells exhibiting neurites two times the length of the cell body were deemed differentiated. To reveal the differentiation percentages, the numbers of differentiated cells were divided by the total number of cells. Percentages were taken from TABLE 5. Mev or M=mevinolin, CD= 2-hydroxypropyl-β-cyclodextrin, Chol+EtOH=cholesterol in ethanol, CD+Chol= 2-hydroxypropyl-β-cyclodextrin loaded with cholesterol.
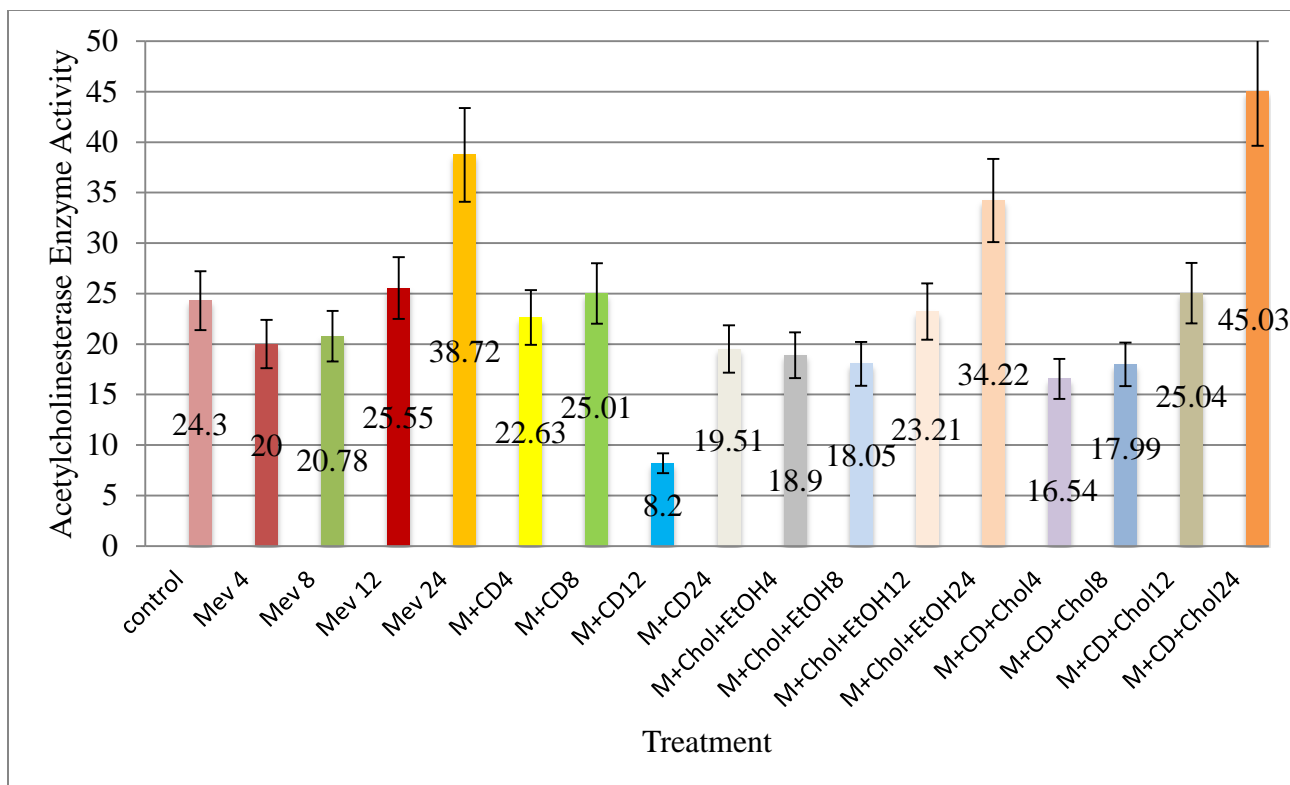
Figure 21. The impact of mevinolin supplemented with 2-hydroxypropyl-β-cyclodextrin, cholesterol in ethanol, or 2-hydroxypropyl-β-cyclodextrin loaded with cholesterol on the acetylcholinesterase activity. Cells were grown in 100mm dishes in culture medium and incubated. Upon reaching 60-70% confluence, cells received mevinolin (10μM) and mevinolin (10μM) + (1mM) cholesterol in ethanol treatments administered directly to the culture medium. Mevinolin (10μM) + 2-hydroxypropyl-β-cyclodextrin (10mM) and mevinolin (10μM) + 2-hydroxypropyl-β-cyclodextrin (10mM) + cholesterol (1mM) treatments were performed as media exchanges. After treatments, dishes were incubated. After indicated times shown in figure, cells were harvested in 0.05M Tris Buffer pH 7.4. Cells were homogenized using dounce homogenizer. Protein concentration of cells lysates were determined using Pierce BCA kit. A modified version of Ellman's assay was performed to determine acetylcholinesterase activity. Protein concentrations were normalized and loaded into 96-well plate along with 0.05M Tris pH 8.0, 4.04×10^{-3} M DTNB, and 8.33×10^{-3} M AThCh. OPTIMax Plate Reader using SoftMaxPro version 2.4.1 software was used to measure AChE activity. Absorbance was measured at 412nm. M=mevinolin, CD=2-hydroxypropyl-β-cyclodextrin, Et+Chol= cholesterol in ethanol, CD+Chol= 2-hydroxypropyl-β-cyclodextrin loaded with cholesterol.

AChE 82 kDa

NeuN 62,
48/46 kDa

MAPK 44/42
kDa

Control — Mev 4 — Mev 8 — Mev 12 — Mev 24 — M+CD 8 — M+CD 12 — M+CD24 — M+Chol 8 — M+Chol 12 — M+Chol 24 — M+CD+Chol 8 — M+CD+Chol 12 — M+CD+Chol 24
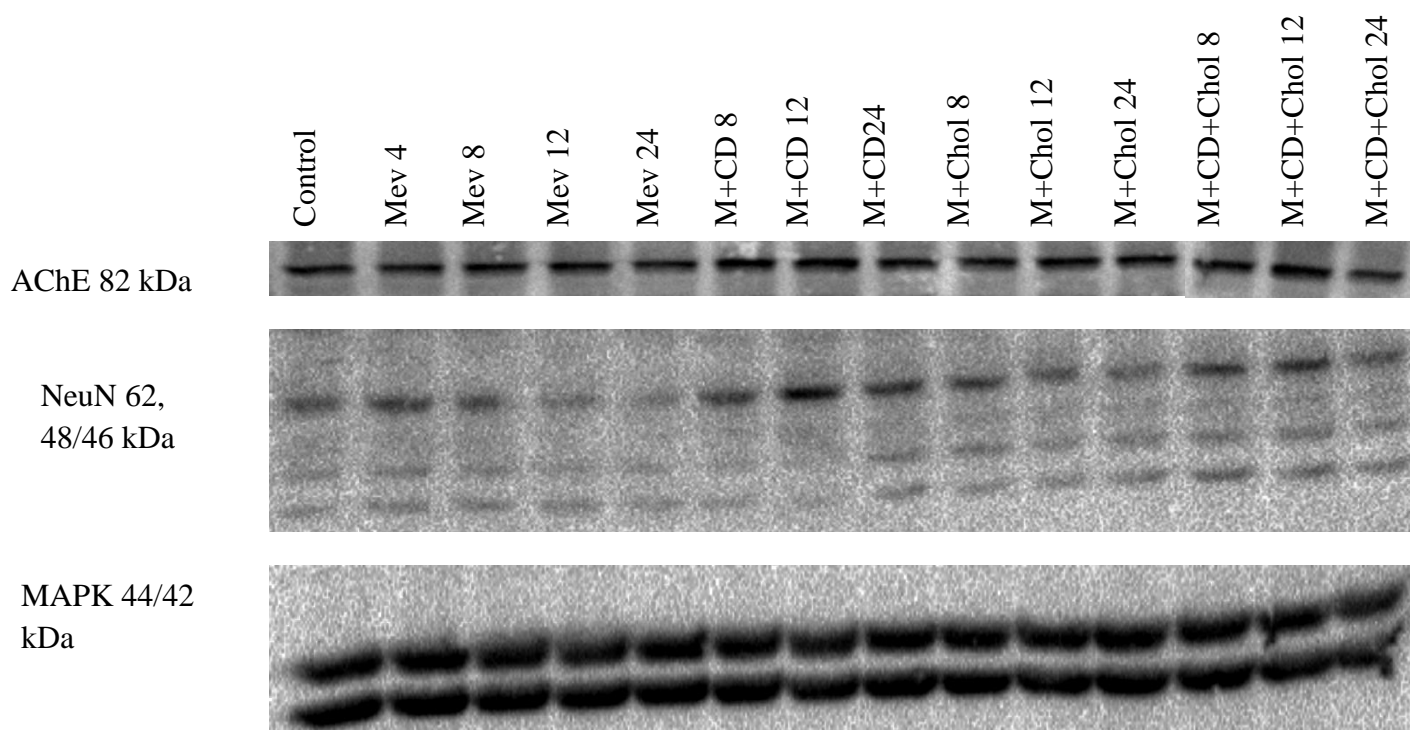
Figure 22. Neuronal protein expression in N2a cells after administration of mevinolin co-treated with 2-hydroxypropyl-β-cyclodextrin, cholesterol in ethanol, cholesterol:CD complex. After indicated times (shown above) cell samples were lysed and 75μg of protein from each sample + loading buffer was separated by 7.5% SDS-PAGE, transferred to PVDF membrane and were western blotted for NeuN, AChE, and MAPK (loading control). To detect proteins, secondary antibodies were conjugated with horseradish peroxidase and visualized with enhanced chemiluminescence. M=mevinolin, CD=2-hydroxypropyl-β-cyclodextrin, Et+Chol= cholesterol in ethanol, CD+Chol= 2-hydroxypropyl-β-cyclodextrin loaded with cholesterol.

DISCUSSION

While most anticancer treatments are non-specific, the new approach to treating cancer with a tumor-specific therapy, by modulating cell differentiation, presents an advancement in the fight against cancer. The flaws in differentiation can be reversed in many cancer cell types providing hope for a specific treatment to achieve terminal cellular differentiation. In this lab study, the role of the cholesterol synthesis pathway was investigated, seeking the causative agent that triggers N2a cell differentiation. The cholesterol synthesis pathway is an important pathway involved in maintaining cellular integrity and cellular health, providing the cell with many crucial bioactive molecules that enable and advance many cellular processes. The biologically active intermediaries of the cholesterol synthesis pathway control signal transduction, cytoskeletal rearrangement, cell communication, proliferation, and membranogenesis. The liver produces most of the body's cholesterol, but the majority of cells retain the ability to synthesize their own cholesterol (Parhami 2002). An amplified activity of the pathway has been credited to facilitating the abnormal growth of cancer cells, indicating the absent regulatory mechanisms. Due to the fact that the cholesterol synthesis pathway regulates cell proliferation and that malignant cells, including neuroblastoma cells, have elevated levels of HMG-CoA reductase indicates that the blocking of the enzyme could potentially lead to a differentiation therapy. This study's investigation of the cholesterol synthesis pathway uses three determining factors of differentiation; morphometric analysis, measurement of the post-synaptic, sympathetic neuron specific enzyme AChE, and the measured expression of neuron specific proteins, AChE and NeuN. The application of

mevinolin treatment to the murine (N2a) neuroblastoma cell triggered differentiation. Consistent with the lab's hypothesis, absence of cholesterol and/or cholesterol intermediates by inhibition of the cholesterol synthesis pathway would trigger differentiation of the (N2a) neuroblastoma cell, potentially providing a differentiation therapy.

This lab's results show the role of the cholesterol synthesis pathway in differentiation of the N2a neuroblastoma. The aggressive blocking of HMG-CoA reductase by mevinolin averts the conversion of HMG-CoA into mevalonate. Statin drugs are used in the treatment for those who suffer from elevated cholesterol levels, preventing cardiovascular disease. The ability of statin drugs to inhibit the cholesterol synthesis pathway has been previously researched amongst multiple cell types: C1300 N2a (Maltese1984), human bladder carcinoma T24 cells (Jakobisiak 1990), (Keyomarsi 1991), PC12 cells (Kumano 2000), myeloma plasma cells RPMI-8226 and U266 (van de Donk 2002), Human ARO anaplastic thyroid cancer cells (Wong 2003), PC12 cells (Schulz 2004), rat hippocampal neurons (Pooler 2006), rat L6 skeletal muscle cells (Martini 2009). Previously published research reveals that mevinolin treatment onto undifferentiated neuroblastoma cells stimulates differentiation, triggering neurite production (Maltese 1984, Maltese 1985). Just as the literature suggest, mevinolin treatment onto the lab's N2a neuroblastoma cells blocked the cholesterol synthesis pathway, triggering differentiation. The optimum differentiation rate was achieved with 10μM mevinolin at 24h post-treatment, triggering an increased production of neurite

outgrowths. When 10μM mevinolin treatment was washed away from N2a cells with cell culture medium, differentiated cells became less prevalent. The decrease in differentiated cells indicated that the N2a cells were able to restart the cholesterol synthesis pathway after 10μM mevinolin removal. The lab's results reveal that differentiated cells did, apparently, undergo dedifferentiation upon mevinolin removal. The dedifferentiation occurred 2h after a post-wash with culture medium. The addition of culture medium was able to restart the cholesterol synthesis pathway, blocking the effects of mevinolin. The ability of proliferation was also seen to decrease, in the presence of mevinolin, implying that the cholesterol synthesis pathway does in fact support N2a cell proliferation.   Morphometric data provides that mevinolin treated cells cannot proliferate, showing sparse amounts of cell growth. The control cells showed increased amount of cell proliferation.

Morphometric analysis of mevalonate added-back onto mevinolin co-treated cells presented a rescued cholesterol synthesis pathway. Mevalonate, the first committed step of the cholesterol synthesis pathway following the action of HMG-CoA reductase, blocked the mevinolin-induced differentiation. The mevalonate add-back restarting the cholesterol synthesis pathway after HMG-CoA reductase inhibition reveals that the observed cellular effects are from mevinolin treatment. Previous experiments that added-back mevalonate onto statin co-treated cells showed blocked cell differentiation amongst multiple cell types: PC12 cells (Fernandez-Hernando 2005), rat hippocampal neurons (Pooler 2006), and human multiple myeloma cells (Holstein 2011).

Malignant growth has often been associated with the extreme presence and

activation of mutated Ras (Swanson 2006, Eisenberg 2008), labeled as "oncogenic Ras,"

has been found in 30% of all cancers in humans (Sleijfer 2005, Schubbert 2007),

implying that the amplification of this specific intermediate was to blame for the

activation of the cancerous state. Rho, Rac, and Cdc42 GTPases are engaged in

cytoskeletal rearrangement progressing to the creation of stress fibers, filopodia and

lamellopodia (Cordle 2005) and are also involved in the cross communication with

signaling pathways involved with oncogenes that influence tumor growth, impacting

survival, proliferation, and development of tumor cells (Malliri 2003). The Rho families

of GTPases have been exposed as playing a critical role in the inducement of

neuritogenesis (Kozma 1997, Katoh 2000). In mevinolin treated cells, G-protein

prenylation is inhibited and cells presented a differentiated state. Interestingly, studies

show that even though the process of prenylation is impeded, GTPases are still activated

due to inability to undergo hydrolysis (Demierre 2005). True to previous outcomes, the

co-treatment of FPP and GGPP intermediates rescued the cholesterol synthesis pathway,

blocking differentiation among other cell types: PC12 cells (Schulz 2004), PC12

(Fernandez-Hernando 2005), rat hippocampal neurons (Pooler 2006), and N2a cells CLL-

131 (Evangelopoulos 2009). Add-back treatment with the non-sterol isoprenoid

intermediates, FPP and GGPP, blocked N2a cell differentiation, blocking the effects of

mevinolin. Both add-back experiments of FPP and GGPP restarted the cholesterol

synthesis pathway, providing that the neuroblastoma cell remains resistant to non-sterol

mediated feedback. The amplified activation of the prenylated proteins (Ras, Rho, Cdc 42, Rac, Rab) have been frequently implicated as the explanation for abnormal growth.

As previously mentioned, amplification of prenylated proteins have been implicated as the inducers of cancer while prior studies have shown that add-back of cholesterol or squalene (the cholesterol precursor) have been found to stimulate differentiation in other cell types: cerebral cortical neurons (Michikawa 1999), HL-60 human promyelocytic cells (Fernandez 2004),and N2a CLL-131 (Evangelopoulos 2009). The two techniques tested in the delivery of cholesterol were cholesterol dissolved in 95% ethanol and the cholesterol:CD complex. The co-treatment of mevinolin and cholesterol (dissolved in 95% ethanol) resulted in a continued triggering of differentiation. At 24h post-treatment, the co-treatment of mevinolin and cholesterol (dissolved in 95% ethanol) triggered differentiation, nearing differentiation rates observed in alone mevinolin treated cells.   Previous add-back studies have not transmitted cholesterol by way of CD, which has been presented as a functional and efficient means of cholesterol delivery (Christian 1997). The co-treatment of mevinolin with the cholesterol:CD complex blocked N2a cell differentiation, blocking neurite outgrowths. The cholesterol:CD complex has been shown to provide a more immediate influx of cholesterol, seemingly transmitting to a sole position in the cell, the plasma membrane (Christian 1997). Previous research has also discovered that when cholesterol is transmitted, by way of CD, the cholesterol molecules turned out to be metabolically active (Christian 1997). Revealed to be competent at drug distribution, the CD core has

been shown not to modify the chemical structure nor the function of bound molecules, as long as the binding strength inside the core remains below $1 \times 10^5 \text{ M}^{-1}$ (Stella 2008). Again, this lab did observe differentiation blocked with the co-treatment of mevinolin and the cholesterol:CD complex. However, this lab no longer trust the results produced from the co-treatment of mevinolin and cholesterol:CD complex. This established method of delivering cholesterol by vehicle is no longer trusted due to the results observed in the co-treatment of mevinolin and CD. The lab hypothesizes that the CD is the problem. In the morphometric analysis, the differentiation rate should have equaled the rate triggered by the alone mevinolin treatment, but the co-treatment of mevinolin and CD showed a decreased rate of differentiation. Lucky to have tested two techniques of cholesterol delivery, this lab observed that the add-back of cholesterol dissolved in ethanol continued to trigger differentiation when co-treated with mevinolin.

The post-synaptic, neuron specific enzyme, AChE, was seen to up-regulate after the inhibition of the cholesterol synthesis pathway. AChE enzyme activity was present in the control cells at low levels. Upon treatment with mevinolin, AChE enzyme activity levels were triggered reaching their maximum at 24h post treatment. Previous studies have shown that AChE enzyme activity levels are upregulated and reach their maximum at 24h post treatment, when treated with mevinolin (Maltese 1984). Co-treatment of mevinolin with mevalonate, FPP, and GGPP triggered reversal of AChE enzyme activity levels, reaching levels found in the control cells. Both cholesterol (dissolved in 95% ethanol and cholesterol:CD complex) co-treated with mevinolin showed decreased AChE

enzyme activity at early times (4h-12h). At 24h post treatment, both cholesterol add-back treatments saw AChE enzyme activity levels climax to levels of mevinolin treated cells. The co-treatment of mevinolin with cholesterol dissolved in 95% ethanol and the co-treatment of mevinolin and the cholesterol:CD complex, blocks differentiation at early times, but does not block differentiation at 24h post-treatment. The increased activity of AChE enzyme presents a differentiated cell at 24h post-treatment. The confusing aspect is that the up-regulated AChE enzyme activity in the cells co-treated with mevinolin and cholesterol:CD complex did not correlate with increased neurite outgrowths. The add-back with cholesterol:CD complex treatment triggered cells to act differentiated but not look differentiated. The add-back of cholesterol dissolved in 95% ethanol showed increased differentiation rates, as shown in morphometric analysis, nearly reaching the mevinolin treated cells, while also triggering an up-regulation of AChE enzyme activity.

This lab's differentiation study further shows the increased expression of neuron specific proteins in the neuroblastoma cell after treatment with mevinolin. Mevinolin induced differentiation of the N2a neuroblastoma cell triggered an upregulation of AChE and NeuN. The neuron specific proteins were expressed in a time dependent manner, after 10μM mevinolin treatment, with full expression at 24h post treatment. Previous studies show that the onset of neuronal cell differentiation is accompanied with an increased expression of NeuN (Lind 2005, Evangelopoulos 2009) and AChE (Anderson 2007). When mevinolin co-treated cells with mevalonate, FPP, GGPP, and cholesterol, each of the intermediates regulates the effects of mevinolin, decreasing the expression of

neuronal proteins. The add-back experiments results signify blocking of differentiation

due to the restarting of the cholesterol synthesis pathway.

After viewing neuroblastoma differentiation by the elimination of the cholesterol

synthesis pathway, it became of interest to discover where along the pathway remains the

agent(s) of differentiation that would induce the N2a neuroblastoma cells to differentiate.

The lab shows a thorough investigation of cellular differentiation through the cholesterol

synthesis pathway. Previous research of the cholesterol synthesis pathway presents

limited differentiation studies, observing few intermediates and proposed terminal

differentiation through limited differentiation determinants. This study, however,

examines the entire cholesterol synthesis pathway, investigating multiple biologically

active intermediates and their role in differentiation. Specifically, this is the first study to

use multiple differentiation determinants to determine terminal differentiation of the N2a

neuroblastoma.   The strengths of this differentiation study are that terminal

differentiation was determined by three factors; morphometric analysis, measurement of

the post-synaptic, sympathetic, neuron specific enzyme, AChE, and expression of neuron

specific proteins, AChE and NeuN. This lab applied each differentiation determinant to

each intermediate add-back to determine the extent of N2a differentiation. By these

determinants we were able to determine if N2a cells had undergone terminal

differentiation or failed to differentiate. Treatment with mevinolin saw the N2a cells

terminally differentiate.   Mevinolin co-treatment with mevalonate, FPP, and GGPP

completely blocked cellular differentiation. These intermediates failed to trigger

differentiation, not reaching levels seen in mevinolin treated cells. The add-back

experiments with these biologically active intermediates blocked differentiation,

inhibiting neurite outgrowths, dramatically inhibiting AChE enzyme activity production,

as well as decreasing the expression of neuron-specific proteins, NeuN and AChE. The

add-back of cholesterol (dissolved in 95% ethanol) triggered N2a neuroblastoma cell

differentiation by triggering neurite outgrowths, up-regulating AChE enzyme activity,

and the expression of neuron specific proteins, AChE and NeuN.

CONCLUSION

The summation of our study demonstrates that inhibition of the cholesterol synthesis pathway subdues malignant growth, inducing a differentiated cell. These results illustrate the significance of the cholesterol synthesis pathway and the focus the pathway deserves as being a differentiation therapy target. The lab also presents the role of intermediates of the cholesterol synthesis pathway in the differentiation of the N2a neuroblastoma cell, while in search for the agent(s) of differentiation. Based on the lab's results, the differentiation agent(s) rest above cholesterol production in the cholesterol synthesis pathway. Future differentiation agent studies should focus on the add-back of intermediates that precede the production of cholesterol, specifically between squalene and lanosterol, to determine their role in differentiation. Differentiation therapies are still in the early stages of cancer treatment, but the use of a differentiation agent in combination with statins as a multi-drug therapy shows promise as a cancer specific treatment.

APPENDIX

MEDIA, SOLUTIONS, AND BUFFERS

Culture Medium
       500ml Dulbecco's Modified Eagle's Medium/Ham's F-12 50/50
       55ml Fetal Bovine Serum (FBS)
       5ml 10,000 I.U. Penicillin; 10,000μg/mL Streptomycin
       5ml Vitamins 100XSolution

Freeze-down Media
       90% culture medium
       10% Dimethyl Sulfoxide (DMSO)

0% FBS Dilution Media
       500ml Dulbecco's Modified Eagle's Medium/Ham's F-12 50/50
       5ml 10,000 I.U. Penicillin; 10,000μg/mL Streptomycin
       5ml Vitamins 100X Solution

Trypsin EDTA 1X, 0.25% Trypsin/2.21mM EDTA

Ca++ free, Mg++ 1X Phosphate Buffered Saline (PBS)

Buffer pH 8.0 Tris Base 0.05M
       1.82g Tris Base
       300mL dH$_2$O
       pH to 8.0

Buffer pH 7.4 Tris Base 0.05M
       1.82g Tris Base
       300mL dH$_2$O
       pH to 7.4

4.04×10^{-3} M DTNB (5, 5-dithio(bis-2-nitrobenzoic acid))
       16.0mg DTNB
       9mL 7.4 Tris Base Buffer
       Add NaOH (5 drops)
       QS to 10mL with 7.4 Tris Base Buffer

8.33×10^{-3}M AThCh (Acetylthiocholine iodide salt)
  24.1mg AThCh
  10mL dH_2O

7.5% Polyacrylamide Gel (Separation Gel)
  7.5ml Protogel
  7.5ml 1.5M Tris Base pH 8.8
  15ml distilled H_2O
  36μl of TEMED
  112.5μl APS

Stacking Gel
  1.0ml Protogel
  2.5ml 0.5M Tris (pH 6.8)
  6.4ml dH_2O
  100μl 10% SDS
  12μl TEMED
  37.5μl APS

Electrode Buffer (10X) 2L
  60gm Tris Base
  288gm Glycine
  20gm SDS or 100ml 20% SDS

TBS-T 10X
  .25 M Tris, pH 8.6 (30.3g)
  1.25 M NaCl (78.05g)
  pH to 8.0 before adding Tween
  1% TWEEN

TBS-T 1X
  Dilution 1:10
  100ml TBS-T 10X
  900ml dH_2O

Transfer Buffer 10X
  116g Glycine
  232.2g Tris Base
  14.8g SDS
  Add to 2L of dH_2O mix then QS to 4L

29g Glycine
58.05g Tris Base
3.7g SDS
Add to 500mL of dH_2O mix then QS to 1L

Transfer Buffer 1X
  4L = 400mL 10X TB
      800mL Methanol
      2.8L dH_2O

  3L = 300mL 10X TB
      600mL Methanol
      2.1 L dH_2O

  2L = 200mL 10X TB
      400mL Methanol
      1.4 L dH_2O

  1L = 100mL 10X TB
      200mL Methanol
      700mL dH_2O

Loading Buffers
  2X
  6ml 10% SDS
  6.6ml 0.5M Tris pH 6.8
  13.0ml 100% glycerol
  24.4ml H_2O
  0.2g bromophenol blue

  3X
  9ml 10% SDS
  10ml 0.5M Tris pH 6.8
  20ml 100% glycerol
  11ml H_2O
  0.2g bromophenol blue

  4X
  12ml 10% SDS
  13.2ml 0.5M Tris pH 6.8
  26ml 100% glycerol
  0.2g bromophenol blue

100% Beta-mercaptoethanol

4% nonfat milk
    8g nonfat dry milk
    200ml 1X TBS-T

1% nonfat milk (100ml)
    25ml 4% nonfat milk
    75ml 1X TBS-T

Mevinolin--- MW 404.54
    Dissolved in 2.5ml DMSO---24.7mM Stock Solution
    Diluted (1:10) in culture medium (0%FBS)--- 2.47mM

Mevalonolactone---MW 130.14
    0.726 M Stock Solution
    Diltued (1:24) in culture medium (0%FBS)--- 29.04mM

Farnesyl Pyrophosphate Ammonium Salt--- MW 433.42

Geranylgeranyl Pyrophosphate Ammonium Salt---MW 450.44

Cholesterol---MW 386.66
    Dissolved in 95% ethanol---20mM stock solution
    Diluted in culture medium (10% FBS)---143µM

2-hydroxypropyl-β-cyclodextrin----MW 1396
    Dissolved in culture medium(10% FBS)---10mM

Lysis Buffer
    Cell Lytic Reagent--500µl
    100mM EDTA
    0.2M Sodium Vanadate
    1% Protease inhibitor cocktail

LITERATURE CITED

Adams Christopher M, Reitz Julian DeBrabander Jef K, Feramisco Jamison D, Li Lu, Brown Michael S, Goldstein Joseph L. 2004. Cholesterol and 25-Hydroxycholesterol Inhibit activation of SREBPs by different Mechanisms, Both Involving SCAP and Insigs. The Journal of Biological Chemistry. 279(50): 52772-52780.

Adjei Alex A. 2001. Blocking Oncogenic Ras Signaling for Cancer Therapy. Journal of the National Cancer Institute. 93(14): 1062-1074.

Aznar Salvador, Fernandez-Valeron Pilar, Espina Carolina, Lacal Juan Carlos. 2004. Rho GTPases: potential candidates for anticancer therapy. Cancer Letters. 206: 181-191.

Brodeur GM. 2003. NEUROBLASTOMA: BIOLOGICAL INSIGHTS INTO A CLINICAL ENIGMA. Nature Reviews Cancer. 3(3): 203-216.
Buchwald HH. 1992. Cholesterol inhibition, cancer, and chemotherapy. Lancet. 339: 1154-1156.

Buhaescu I, Izzedine H. 2007. Mevalonate pathway: a review of clinical and therapeutical implications. Clinical Biochemistry 40: 575-584.

Chan KKW, Oza AM, Siu LL. 2003. The statins as Anticancer Agents. Clinical Cancer Research. 9: 10-19.

Christian Aimee E., Haynes M. Page, Phillips Michael C., Rothblat George H. 1997. Use of cyclodextrins for manipulating cellular cholesterol content. Journal of Lipid Research. 38: 2264-2272.

Cohen David C., Massoglia Sharon L., Gospodarowicz Denis. 1982. Feedback Regulation of 3-Hydroxy-3-methylglutaryl Coenzyme A Reductase in Vascular Endothelial Cells. THE JOURNAL OF BIOLOGICAL CHEMISTRY. 257(18): 11106-11112.

Cordle Andrew, Koenigsknect-Talboo Jessica, Wilkinson Brandy, Limpert Allison, Landreth Gary. 2005. Mechanisms of Statin-mediated Inhibition of Small G-protein Function. THE JOURNAL OF BIOLOGICAL CHEMISTRY. 280(40): 34202-34209.

Dawson Paul A., Metherall James E., Ridgway Neale D., Brown Michael S., Goldstein Joseph L. 1991. THE JOURNAL OF BIOLOGICAL CHEMISTRY. 266(14): 9120-9134.

Debose-Boyd RA. 2008. Feedback Regulation of Cholesterol synthesis: sterolaccelerated ubiquitination and degradation of HMG CoA reductase. Cell Research. 18: 609-621.

Demierre MF, Higgins PDR, Gruber SB, Hawk E, Lippman SM. 2005. STATINS AND CANCER PREVENTION. Nature Reviews Cancer. 5: 930-942.

Dhir Sunita, Wheeler Kate. 2010. Neonatal Neuroblastoma. Early Human Development. 86: 601-605.

Edjso A, Holmquist L, Pahlman S. 2007. Neuroblastoma as an experimental model for neuronal differentiation and hypoxia-induced tumor cell dedifferentiation. Seminars in Cancer Biology. 17: 248-256.

Eisenberg Sharon, Henis Yoav I. 2008. Interactions of Ras proteins with the plasma membrane and their roles in signaling. Cellular Signalling. 20: 31-39.

Ellman George L., Courtney K. Diane, Andres Jr. Valentino, Featherstone Robert M. 1961. A NEW AND RAPID COLORMETRIC DETERMINATION OF ACETYLCHOLINESTERASE ACTIVITY. Biochemical Pharacology. 7: 88-95.

Evangelopoulos ME, Weis J, Kruttgen A. 2005. Signalling pathways leading to neurobalstoma differentiation after serum withdrawal: HDL blocks neuroblastoma differentiation by inhibition of EGFR. Oncogene. 24: 3309-3318.

Evangelopoulos ME, Weis J, Kruttgen A. 2009. Mevastatin-Induced Neurite Outgrowth of Neurobalstoma Cells via activation of EGFR. Journal of Neuroscience Research 87: 2138-2144.

Fernandez Carlos, Lobo Maria del Val T., Gomez-Coronado Diego, Lasuncion Miguel A. 2004. Cholesterol is essential for mitosis progression and its defiency induces polypliod cell formation. Experimental Cell Research. 300: 109-120.

Fernandez Carlos, Martin Miguel, Gomez-Coronado Diego, Lasuncion Miguel A. 2005. Effects of distal cholesterol biosynthesis inhibitors on cell proliferation and cell cycle progression. Journal of Lipid Research. 46: 920-929.

Fernandez-Hernando, Suarez Yajaira, Lasuncion Miguel A. 2005. Lovastatin-induced PC-12 cell differentiation is associated with RhoA/RhoA kinase pathway activation. Molecular and Cellular Neuroscience. 29: 591-602.

Fisher Jonathan P. H., Tweddle Deborah A. 2012. Neonatal neuroblastoma. Seminars in Fetal & Neonatal Medicine. 17: 207-215.

Funfschilling Ursula, Jockusch Wolf J., Sivakumar Nandhini, Mobius Wiebke, Corthals Kristina, Li Sai, Quintes Susanne, Kim Younghoon, Schaap Iwan A. T., Rhee Jeong-Seop, Nave Klaus-Armin, Saher Gesine. 2012. Critical Time Window of Neuronal Cholesterol Synthesis during Neurite Outgrowth. The Journal of Neuroscience. 32(22): 7632-7645.

Gill Saloni, Chow Renee, Brown Andrew J. 2008. Sterol regulators of cholesterol homeostasis and beyond: The oxysterol hypothesis revisited and revised. Progress in Lipid Research. 47: 391-404.

Holstein Sara A, Hohl Raymond J. 2011. Isoprenoid biosynthetic pathway inhibition disrupts monoclonal protein secretion and induces the unfolded protein response pathway in multiple myeloma cells. Leukemia Research. 35: 551-559.

Ilangumaran Subburaj, Hoessli Daniel C. 1998. Effects of cholesterol depletion by cyclodextrin on the spingolipid microdomains of the plasma membrane. Biochemical Journal. 335: 433-440.

Jakobisiak Marek, Bruno Silvia, Skierski Janusz S., Darzynkiewicz Zbigniew. 1991. Cell cycle specific effects of lovastatin. Proceedings of the National Academy of Science. 88: 3628-3632.

Johnson Glynis, Moore Samuel W. 2003. Human acetylcholinesterase binds to laminin-1 and human collagen IV by an electrostatic mechanism at the peripheral anionic site. Neuroscience Letters. 337: 37-40.

Katoh Hironori, Yasui Hidekazu, Yamaguchi Yoshiaki, Aoki Junko, Fujita Hirotada, Mori Kazutoshi, Negishi Manabu. 2000. Small GTPase RhoG Is a Key Regulator for Neurite Outgrowth in PC12 Cells. Molecular and Cell Biology. 20(19): 7378-7387.

Keyomarsi Khandan, Sandoval Larue, Band Vimla, Pardee Arthur B. 1991. Synchronization of Tumor and Normal Cells from G_1 to Multiple Cell Cycles by Lovastatin. CANCER RESEARCH. 51: 3602-3609.

Kim Kee K, Adelstein Robert S, Kawamoto Sachiyo. 2009. Identification of Neuronal Nuclei (NeuN) as Fox-3, a New Member of the Fox-1 Gene Family of Splicing Factors. The Journal of Biological Chemistry. 284(45): 31052-31061.

Koenigsberger C., Chiappa S., Brimijoin S. 1997. Neurite Differentiation Is Modulated in Neuroblastoma Cells Engineered for Altered Acetylcholinesterase Expression. Journal of Neurochemistry. 69: 1389-1397.

Kozma Robert, Sarner Shula, Ahmed Sohail, Lim Louis. 1997. Rho Family GTPases and Neuronal Growth Cone Remodeling: Relationship between Increased Complexity Induced by Cdc42Hs, Rac1 and Acetylcholine and Collapse Induced by RhoA and Lysophosphatidic Acid. MOLECULAR AND CELL BIOLOGY. 17(3): 1201-1211.

Kuipers HK, van den Elsen P. 2007. Immunomodulation by statins: Inhibition of cholesterol vs. isoprenoid biosynthesis. Biomedicine & Pharmacotherapy 61: 400-407.

Kumano T, Mutoh T, Nakagawa H, Kuriyama M. 2000. HMG-CoA reductase inhibitors induces a transient growth factor receptor, Trk, and morphological differentiation with fatal outcome in PC12 cells. Brain Research. 859: 169-172.

Leszczyniecka Magdalena, Roberts Terry, Dent Paul. Grant Steven, Fisher Paul B. 2001. Differentiation therapy of human cancer: basic science and clinical applications. Pharmacology & Therapeutics. 90: 105-156.

Lind D, Franken S, Kappler J, Jankowski J, Schilling K. 2005. Characterization of the Neuronal Marker NeuN as a Multiply Phosphorylated Antigen With Discrete Subcellular Localization. Journal of Neuroscience Research. 79: 295-302.

Malliri Angeliki, Collard John G. 2003. Role of Rho-family proteins in cell adhesion and cancer. Current Opinion in Cell Biology. 15: 583-589.

Maltese WA. 1984. INDUCTION OF DIFFERENTIATION IN MURINE NEUROBLASTOMACELLS BY MEVINOLIN, A COMPETITIVE INHIBITOR OF 3-HYDROXY-3-METHYLGLUTARYL COENZYME A REDUCTASE. BIOCHEMICAL AND BIOPHYSICAL RESEARCH COMMUNICATIONS. 120(2): 454-460.

Maltese William A., Defendini Richard. Green Robert A., Sheridan Kathleen M., Donley Diane K. 1985. Suppression of Murine Neuroblastoma Growth In vivo by

Mevinolin, a competitive Inhibitor of 3-Hydroxy-3-methylglutaryl-Coenzyme A Reductase. Journal of Clinical Investigation. 76(5): 1748-1754.

Maris JM, Matthay KK. 1999. Molecular Biology of Neuroblastoma. Journal of Clinical Oncology 17 (7): 2264-2279.

Martini C, Trapani L, Narciso L, Marino M, Trentalance A, Pallottini V. 2009. 3-hydroxy 3-methylglutaryl Coenzyme A Reductase Increase Is essential for Rat Muscle Differentiation. Journal of Cellular Physiology. 220: 524-530.

Michikawa Makoto, Yanagisawa Katsuhiko. 1999. Inhibition of Cholesterol Production but Not of Nonsterol Isoprenoid Products Induces Neuronal Cell Death. Journal of Neurochemistry. 72: 2278-2285.

Mo Huanbiao, Elson Charles E. 2004. Studies of the Isoprenoid-Mediated Inhibition of Mevalonate Synthesis Applied to Cancer Chemotherapy and Chemoprevention. Experimental Biology and Medicine. 229: 567-585.

Nakanish Mahito, Goldstein Joseph L., Brown Michael S. 1988. Multivalent Control of 3-Hydroxy-3methylglutaryl Coenzyme A reductase. THE JOURNAL OF BIOLOGICAL CHEMISTRY. 263(18): 8929-8937.

Nishimura Taki, Inoue Takao, Shibata Norihito, Sekine Azusa, Takabe Wakako, Noguchi Noriko, Arai Hiroyuki. 2005. Inhibition of cholesterol biosynthesis by 25-hydroxycholesterol is independent of OSBP. Genes to Cells. 2005: 793-801.

Parhami Farhad, Mody Nilam, Gharavi Nima, Ballard Alex J, Tintut Yin, Demer Linda L. 2002. Role of the Cholesterol Biosynthetic Pathway in Osteoblastic Differentiation of Marrow Stromal Cells. Journal of Bone and Mineral Research. 17: 1997-2003.

Paraoanu Laura E., Layer Paul G. 2004. Mouse acetylcholinesterase interacts in yeast with the extracellular matrix component laminin-1β. FEBS Letters. 576: 161-164.

Paraoanu LE, Layer PG. 2008. Acetylcholineesterase in cell adhesion, neurite growth and network formation. The FEBS Journal. 275: 618-624.

Pons Gerard, O'Dea Robert F, Mirkin Bernard L. 1982. Biological Characterization of the C-1300 Murine Neuroblastoma: An in Vivo Neural Crest Tumor Model. Cancer Research. 42: 3719-3723.

Riley RD, Heney D, Jones DR, Sutton AJ, Lambert PC, Abrams KR, Young B, Wailoo AJ, Burchill SA. 2003. A Systematic Review of Molecular and Biological Tumor Markers in Neuroblastoma. Clinical Cancer Research 10: 4-12

Rudney Harry, Sexton Russell C. 1986. REGULATION OF CHOLESTEROL BIOSYNTHESIS. Annual Review of Nutrition. 6: 245-272.

Sanchez-Martin Carolina C, Davalos Alberto, Martin-Sanchez Covadongo. 2007. Cholesterol Starvation Induces Differentiation of Human Leukemia HL-60 Cells. Cancer Research. 67: 3379-3386.

Sarnat HB, Nochlin D, Born DE. 1998. Neuronal nuclear antigen (NeuN): a marker of neuronal maturation in the early human fetal nervous system. Brain & Development. 20: 88-94.

Schachter Michael. 2004. Chemical, pharmacokinetic and pharmacodynamic properties of statins: an update. Fundamental & Clinical Pharmacology. 19: 117-125.

Schubbert Suzanne, Shannon Kevin, Bollag Gideon. 2007. Hyperactive Ras in development disorders and cancer. NATURE REVIEWS. 7: 295-308.

Schula Joachim G., Bosel Julian, Stoeckel Magali, Megow Dirk, Dirnagl Ulrich, Endres Matthias. 2003. HMG-CoA reductase inhibition causes neurite loss by interfering with geranylgeranylpyrophosphate synthesis. Journal of Neurochemistry. 89: 24-32.

Schwab M, Westermann F, Hero B, Berthold F. 2003. Neuroblastoma: biology and molecular and chromosomal pathology. Oncology 4: 472-480.

Sleijfer Stefan, van der Gaast Ate, Planting Andre S Th, Stoter Gerrit, Verweij Jaap. 2005. The potential of statins as part of anti-cancer treatment. European Journal of Cancer. 41: 516-522.

Slotkin Theodore A, Ryde Ian t, Wrench Nicola, Card Jennifer A, Seidler Frederic J. 2009. Nonenzymatic role of acetylcholinesterase in neurite sprouting: Regional changes in acetylcholinesterase and choline acetyltransferase after neonatal 6-hydroxydopamine lesions. Neurotoxicology and Teratology. 31: 183-186.

Sierra Saleta, Ramos Maria C, Molina Pilar, Esteo Cynthia, Vazquez Jose Antonio, Burgos Javier S. 2011. Statins as Neuroprotectants: A Comparative *In Vitro* Study of Lipophilicity, Blood-Brain-Barrier Penetration, Lowering of Brain Cholesterol, and Decrease of Neuron Cell Death. Journal of Alzheimer's Disease. 23: 307-318

Siperstein Marvin D. 1984. Role of cholesterogenesis and isoprenoid synthesis in DNA replication and cell growth. Journal of Lipid Research. 25: 1462-1468.

Stella Valentino, He Quanren. 2008. Cyclodextrins. Toxicologic Pathology. 36: 30-42.

Swanson Kelly M, Hohl Raymond J. 2006. Anti-Cancer Therapy: Targeting the mevalonate Pathway. Current Cancer Drug Targets. 6: 15-37.

Tong H, Wiemer AJ, Neighbors JD, Hohl RJ. 2008. Quantitative determination of farnesyl and geranylgeranyl diphosphate levels in mammalian tissue. Analytical Biochemistry 378:138-143.

Vamvakopoulos JE. 2005. Three's company: Regulation of Cell Fate by Statins. Current Drug Targets-Cardiovascular & Haematological Disorders. 5: 145-163.

Van Aelst L, D'Souza-Schorey C. 1997. Rho GTPases and signaling networks. Genes & Development. 11: 2295-2322.

van de Donk NWCJ, Kamphuis MMJ, Lokhorst HM, Bloem AC. 2002. The cholesterol lowering drug lovastatin induces cell death in myeloma plasma cells. Leukemia. 16: 1362-1371.

Wang Chih-Yuan, Zhong Wen-Bin, Chang Tien-Chun,Lai Shu-Mei, Tsai Yuan-Feen. 2003. Lovastatin, a3-hydroxy-3-methylglutaryl Coenzyme A Reductase Inhibitor, Induces Apoptosis and Differentiation in Human Anaplastic Thyroid Carcinoma Cells. The Journal of Clinical Endocrinology & Metabolism. 88: 3021-3026.

Wong WW-L, Dimitroulakos J, Minden MD, Penn LZ. 2002. HMG-CoA reductase inhibitors and the malignant cells: the statin family of drugs as triggers of tumor-specific apoptosis. Leukemia. 16: 508-516.